Status of The Fourth Conceptual Detector

Jianchun Wang
IHEP, CAS

CEPC IAC Review, Nov 1-5, 2021

CEPC Detectors in The CDR (I)

Particle Flow Approach
(ILD-like)

3T / 2T
Solenoid Magnet

Yoke + Muon (RPC or μ-RWELL)

LumiCal

Si Pixel Vertex

High granularity
sampling calorimeters

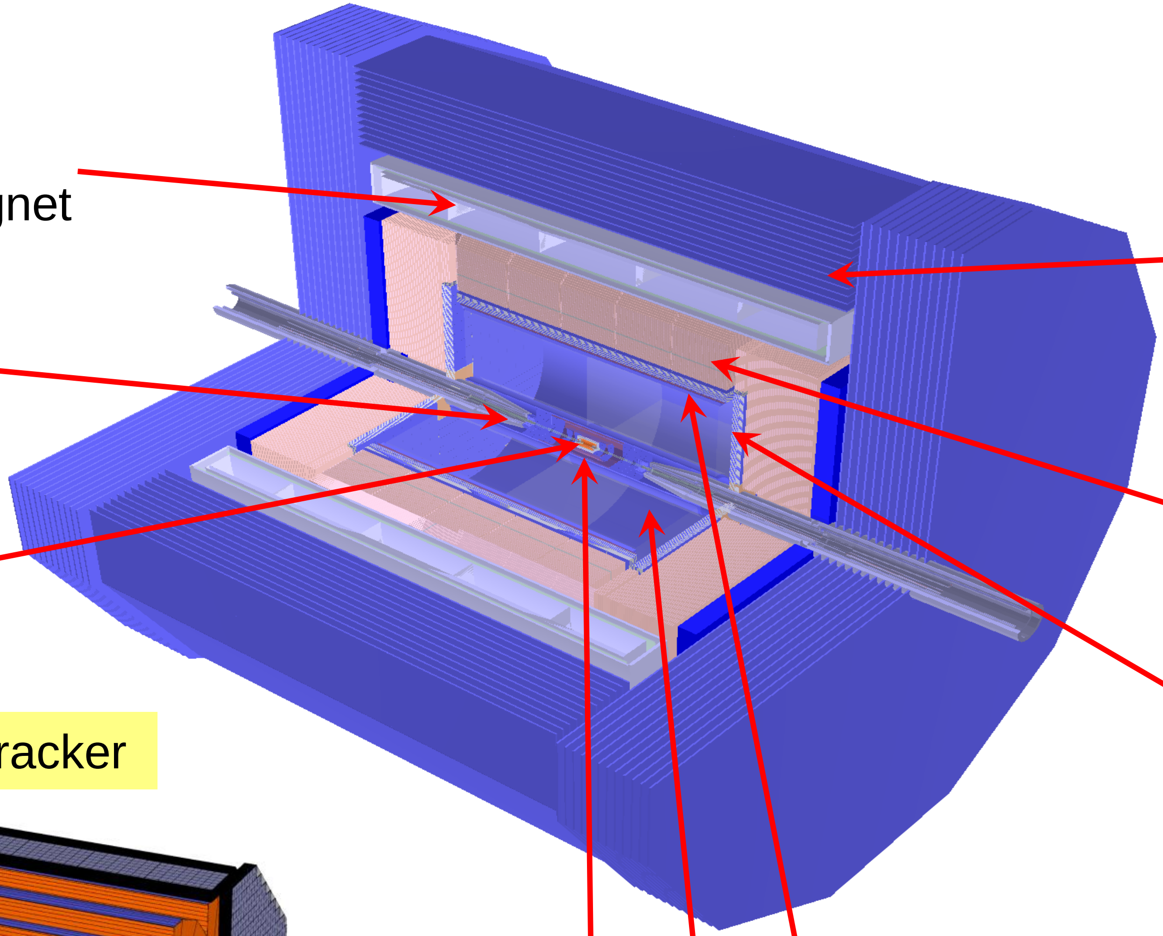

SIT TPC SET
FTD ETD

Full Silicon Tracker

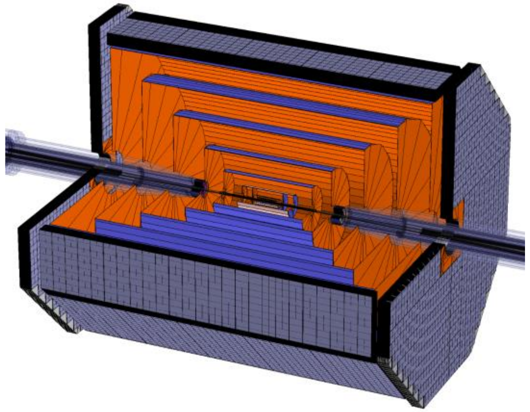

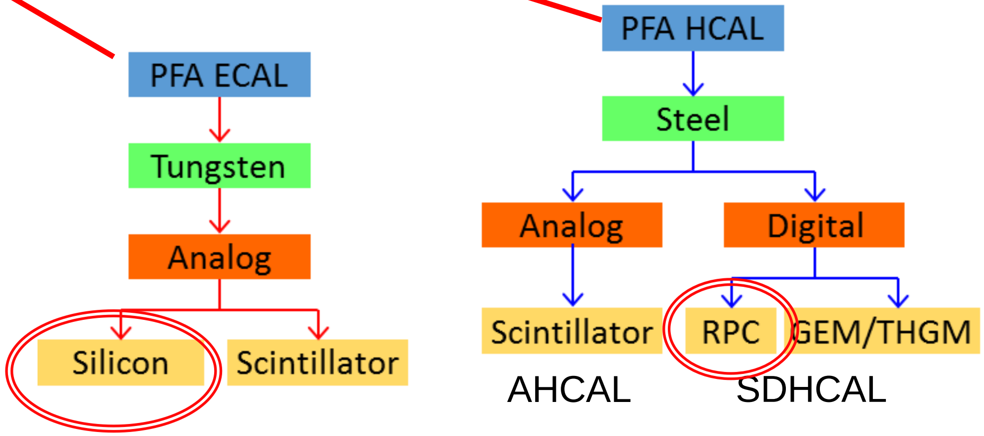

CEPC Detectors in The CDR (II)

IDEA concept
(also proposed for FCC-ee)

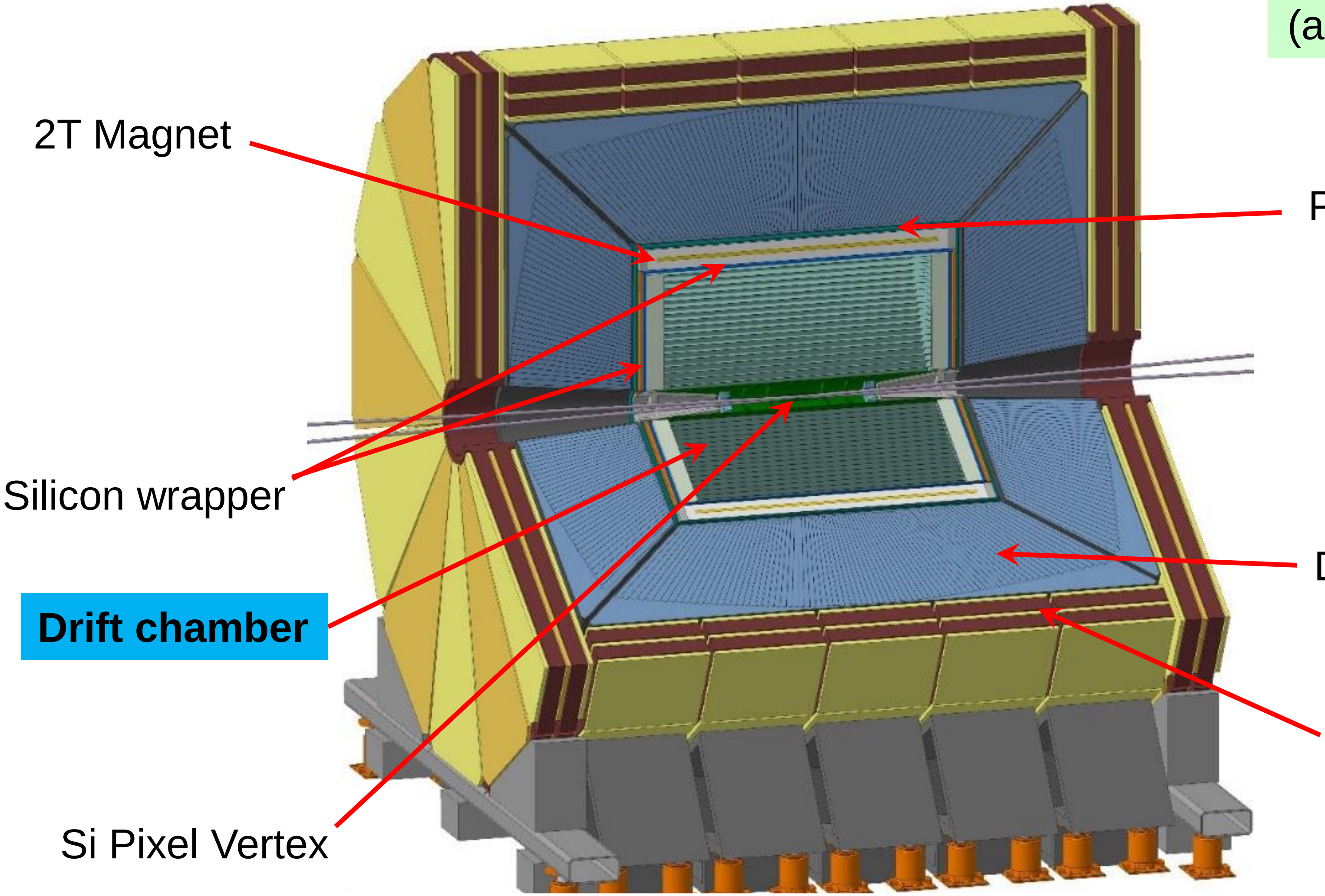

Requirements of The CEPC Detectors

The physics motivations dictate our selection of detector technologies

Physics process	Measurands	Detector subsystem	Performance requirement
$ZH, Z \to e^+e^-, \mu^+\mu^-$ $H \to \mu^+\mu^-$	$m_H, \sigma(ZH)$ $\mathrm{BR}(H \to \mu^+\mu^-)$	Tracker	$\Delta(1/p_T) =$ $2 \times 10^{-5} \oplus \frac{0.001}{p(\mathrm{GeV}) \sin^{3/2}\theta}$
$H \to b\bar{b}/c\bar{c}/gg$	$\mathrm{BR}(H \to b\bar{b}/c\bar{c}/gg)$	Vertex	$\sigma_{r\phi} =$ $5 \oplus \frac{10}{p(\mathrm{GeV}) \times \sin^{3/2}\theta} (\mu\mathrm{m})$
$H \to q\bar{q}, WW^*, ZZ^*$	$\mathrm{BR}(H \to q\bar{q}, WW^*, ZZ^*)$	ECAL HCAL	$\sigma_E^{\mathrm{jet}}/E =$ $3 \sim 4\%$ at 100 GeV
$H \to \gamma\gamma$	$\mathrm{BR}(H \to \gamma\gamma)$	ECAL	$\Delta E/E =$ $\frac{0.20}{\sqrt{E(\mathrm{GeV})}} \oplus 0.01$

- Flavor physics $\Rightarrow$ Excellent PID, better than 2σ separation of π/K at momentum up to ~20 GeV.
- EW measurements $\Rightarrow$ High precision luminosity measurement, $\delta L / L \sim 10^{-4}$.

The 4th Conceptual Detector Design

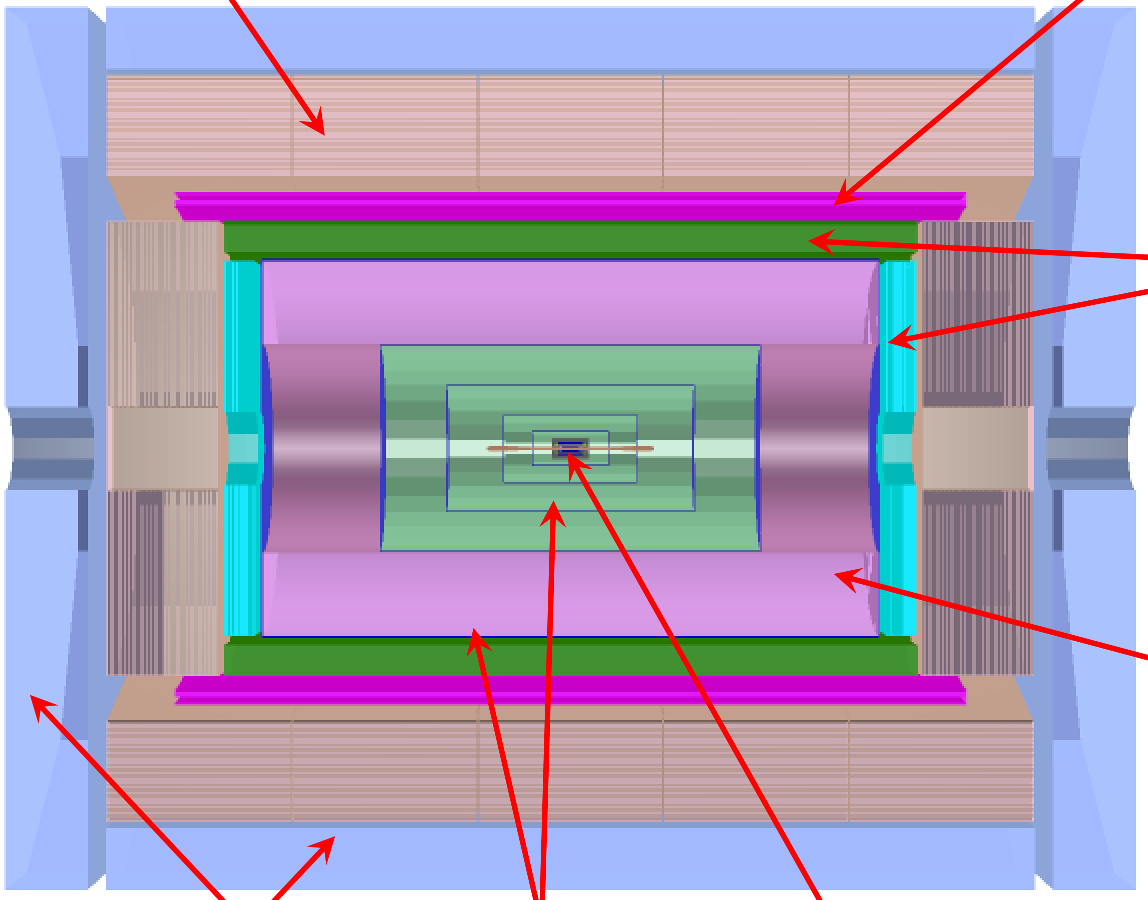

Scint Glass PFA HCAL

Advantage: Cost efficient, high density

Challenges: Light yield, transparency, massive production.

Solenoid Magnet (3T / 2T) Between HCAL & ECAL

Advantage: the HCAL absorbers act as part of the magnet return yoke.

Challenges: thin enough not to affect the jet resolution (e.g. BMR); stability.

Transverse Crystal bar ECAL

Advantage: better π^0/γ reconstruction.

Challenges: minimum number of readout channels; compatible with PFA calorimeter; maintain good jet resolution.

A Drift chamber that is optimized for PID

Advantage: Work at high luminosity Z runs

Challenges: sufficient PID power; thin enough not to affect the moment resolution.

A Drift Chamber
That is Optimized for PID

A Drift Chamber for PID

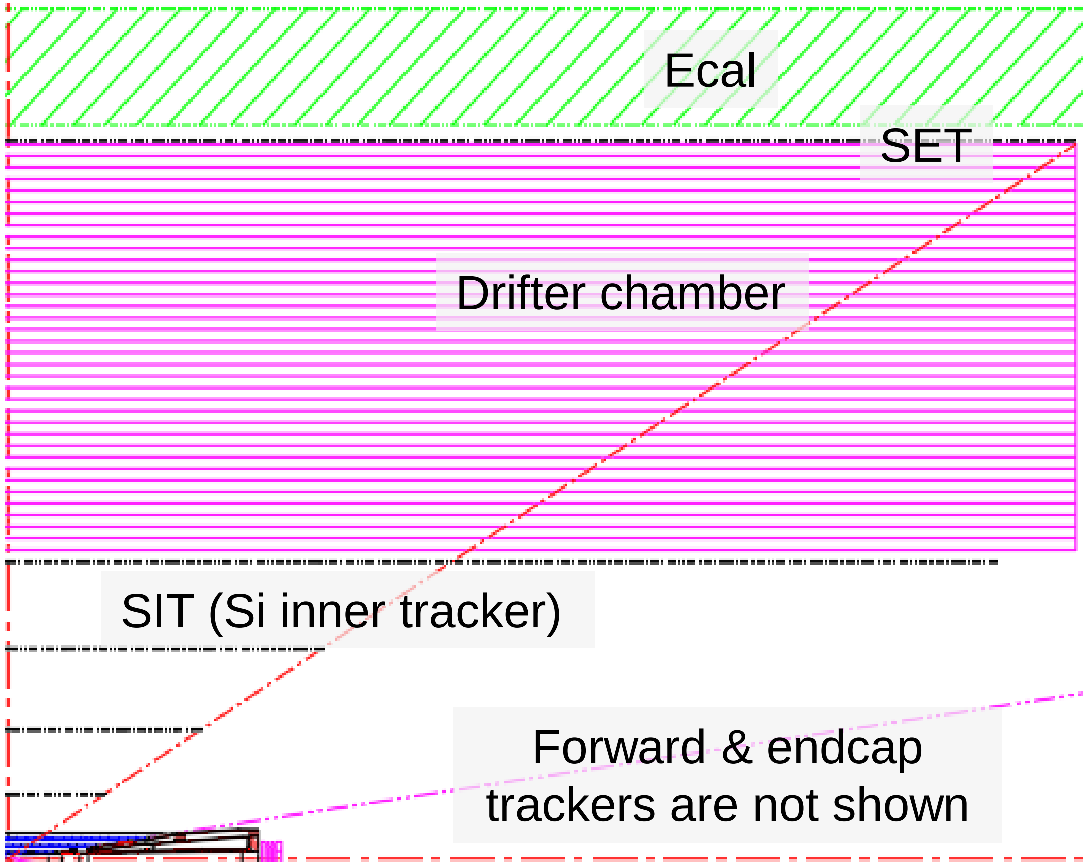

- TPC perform both tracking & PID. But it is a challenge to cope with high luminosity Z runs.
- A Full Silicon Tracker works at high luminosity, but has disadvantage in PID.
- A drift chamber (DC) between the FST layers for >2σ K/π separation (P < 20 GeV).
- It can be optimized specifically for PID, without worrying about its tracking performance.

① Increase the cell size.
② No stereo layers.
③ Maybe slow drift velocity.
④ Optimal # of primary ionization.
⑤ …

PID Using dE/dx vs dN/dx Methods

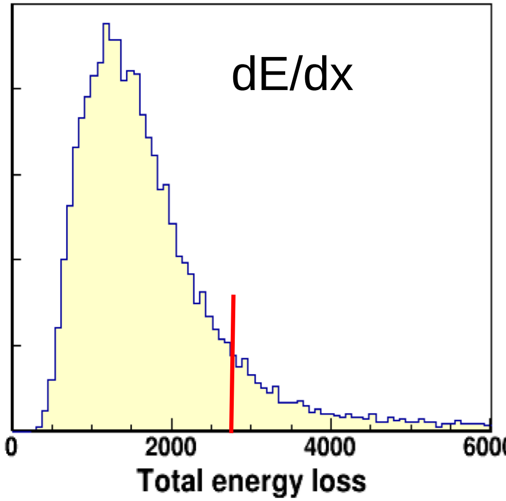

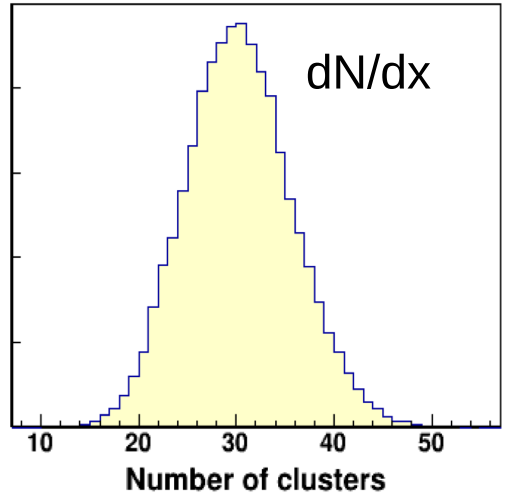

- Conventionally, dE/dx method is used for PID by measuring energy loss over the track length
  - Usually limited to < 10 GeV
  - One limiting factor is the Landau tail
  - Truncated mean leads to a loss of part of the measured information
- Cluster counting method, or dN/dx, measures the number of primary ionizations, which follow Poisson distribution.
  - Less sensitive to Landau tails
  - Significantly improve the separation power

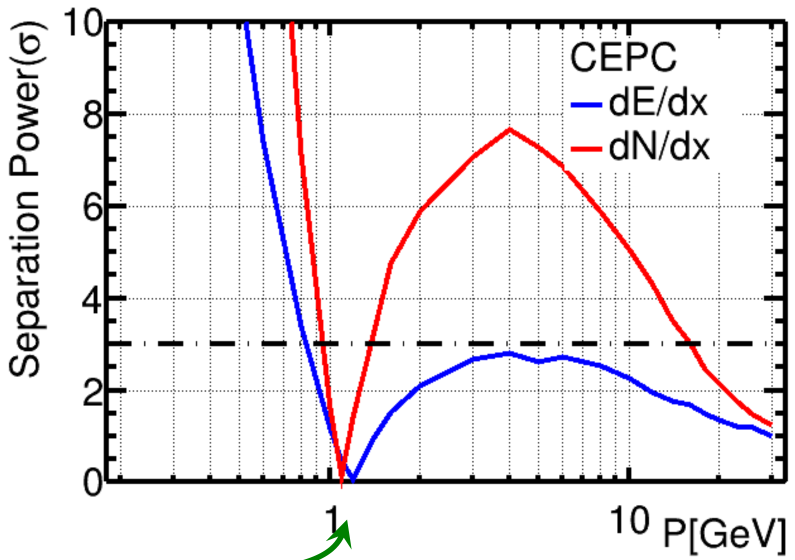

Need a supplementary PID ~ 1 GeV

Key Parameters That Affect PID

- dN/dx resolution: $$\frac{\sigma_{dN/dx}}{dN/dx} \propto \frac{1}{\sqrt{L \cdot \rho_{cl} \cdot \varepsilon}}$$

- PID optimization requirement
  - Long sampling track length L (**Sufficient thickness of DC**)
  - Large primary ionization density ρ_{cl} (**Suitable gas mixture**)
  - High cluster counting efficiency ε (**Fast front-end electronics and low noise**)

- Other concerns
  - Low material budget X/X_0 (minimize the impact of multiple scattering)
  - Location(Inner/Outer radius) (benefit tracking and momentum measurement)

Simulation and Reconstruction of PID Drift Chamber

Induced current from Garfield++

Gas composition: He 90% + iC_4H_{10} 10%
Cell size: 1x1 cm
Particle: 10 GeV/c pions, θ = 90 deg
Average N_{cl}: ~16.5

Simulation of preamplifier

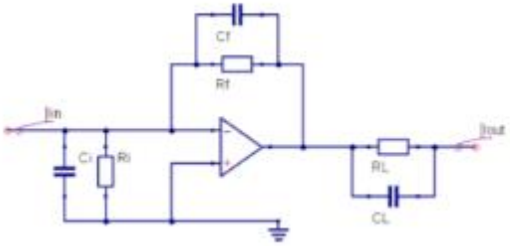

Simulation of noises

- Add white noises to the raw current signal

Peak finding analysis

- Moving average (MA) filter:

$$\mathbf{MA[i]} = \frac{1}{M} \times \sum_{k=0}^{K<M} S[i-k] \text{ (smoothing)}$$

- First difference (D1) filter:

D1[i] = MA[i] – MA[i – 1]

Current [fC / ns]

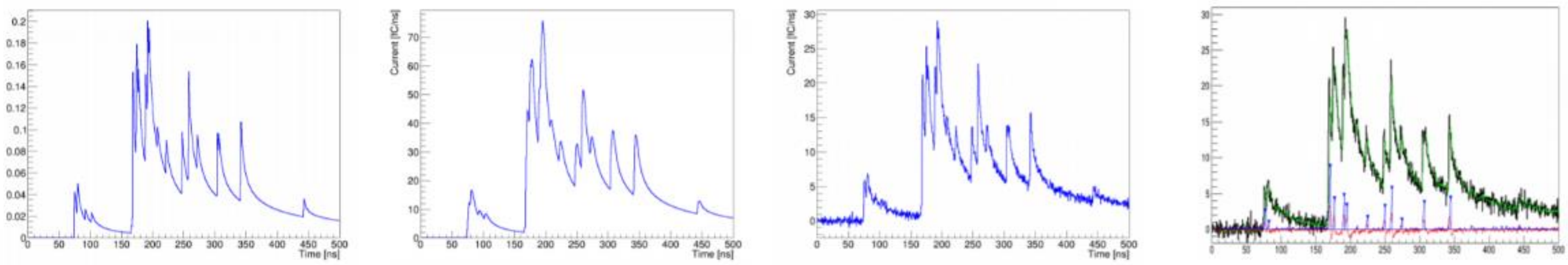

Time [ps]

A joint effort with the IDEA detector study group

K/π Separation Power

Cell size: 1×1 cm^2
Gas mixture: He / iC_4H_{10} (90 / 10)
FE electronics: 2 Gsps

$$S = \frac{\left|\left(\frac{dN}{dx}\right)_\pi - \left(\frac{dN}{dx}\right)_K\right|}{(\sigma_\pi + \sigma_K)/2}$$

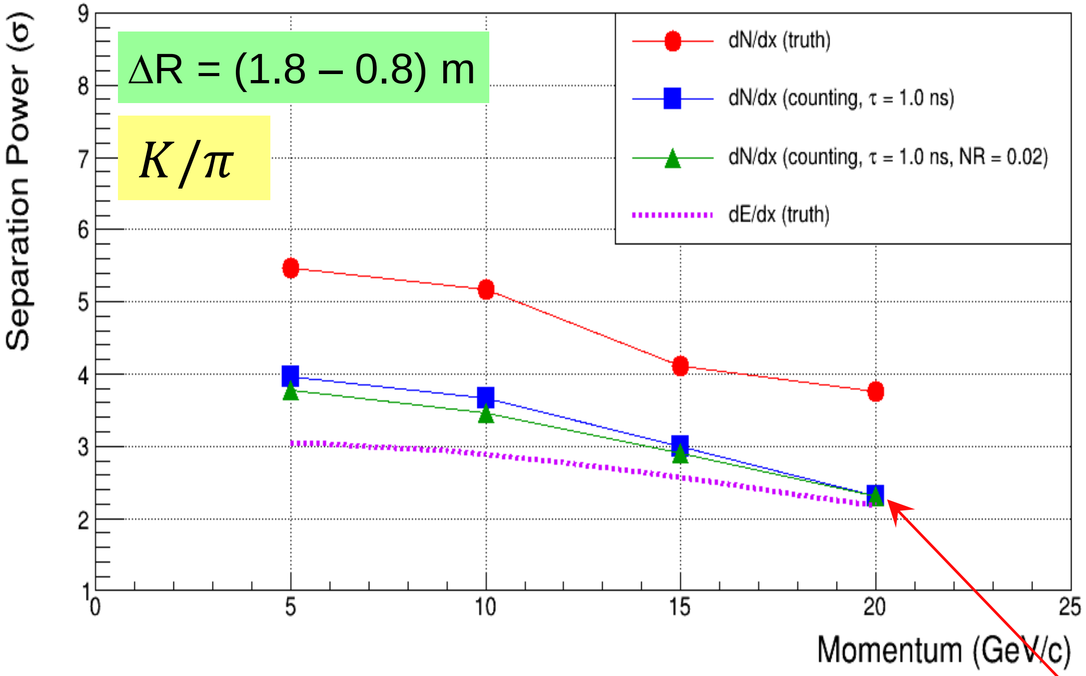

With a simple scaling, a ~80 cm thick drift chamber would deliver 2σ K/π separation at 20 GeV.

PID Efficiency

+ TOF σ_t=50 ps

DC Radius:	(1.8 – 0.8) cm
Gas mixture:	He / iC_4H_{10} (90 / 10)
FE electronics:	2 Gsps

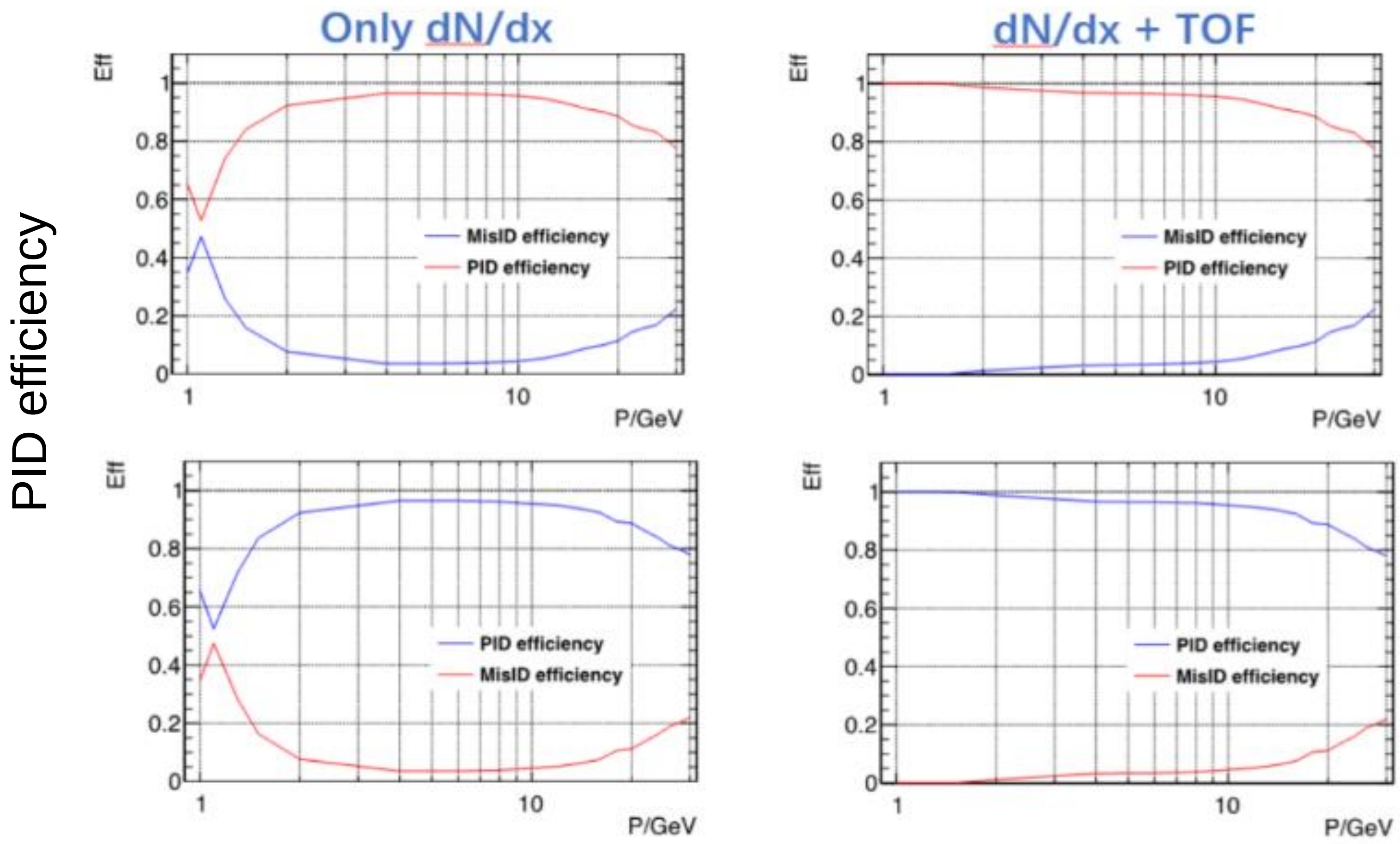

K sample

π sample

For P<20 GeV, K/π PID efficiency > 90% , misidentification rate < 10%

Simulation of Gas Mixture

- To optimize gas mixture
  - High cluster density ρ_{cl} compatibly with the cluster counting efficiency ε
  - Low drift velocity helps identify clusters in time
  - Smaller longitudinal diffusion would benefit both dN/dx measurement and spatial resolution

Cluster density vs ratio of He

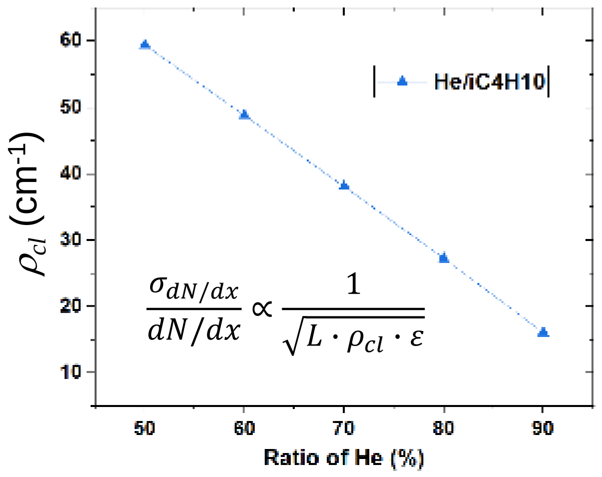

Drift time vs drift distance

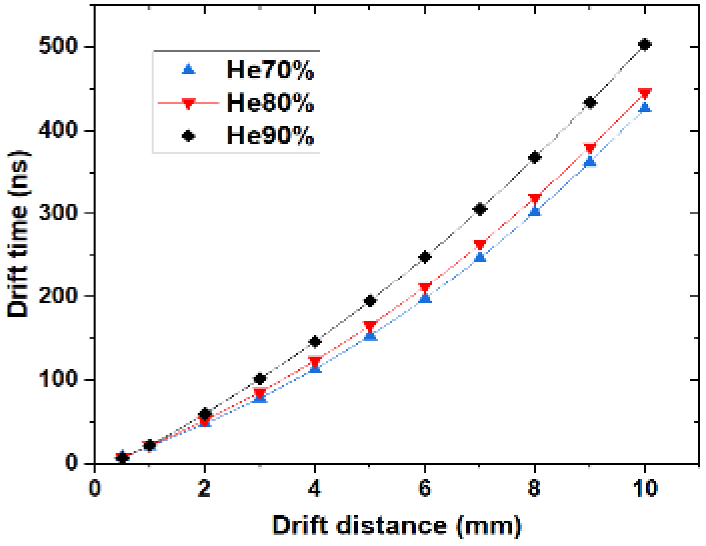

Diffusion effect vs drift distance

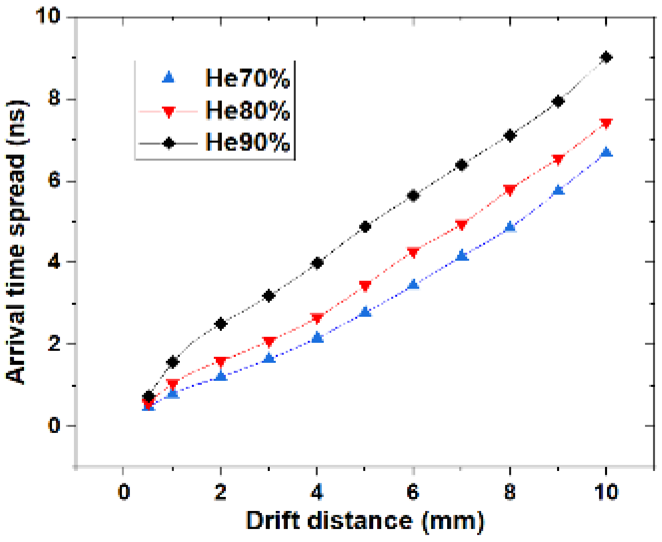

Gain vs H.V.

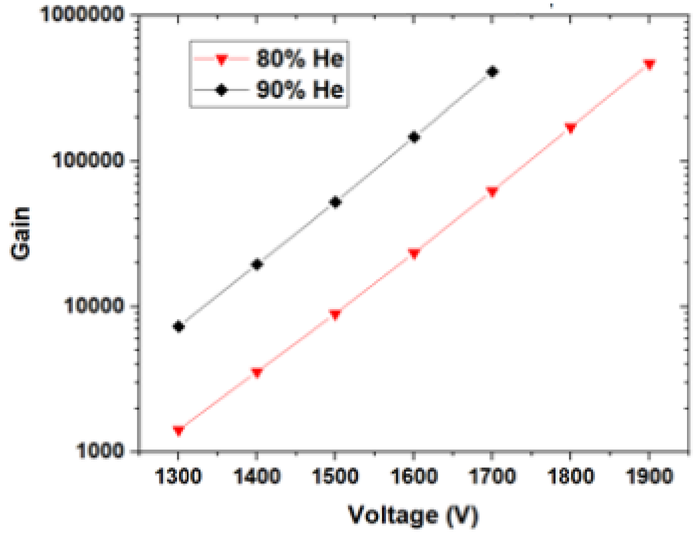

Effects of The Cell Size

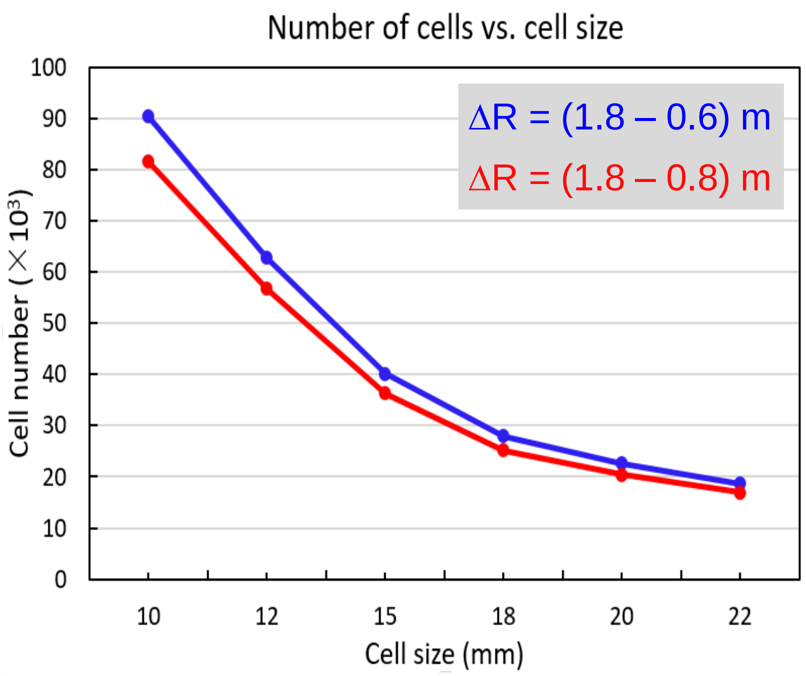

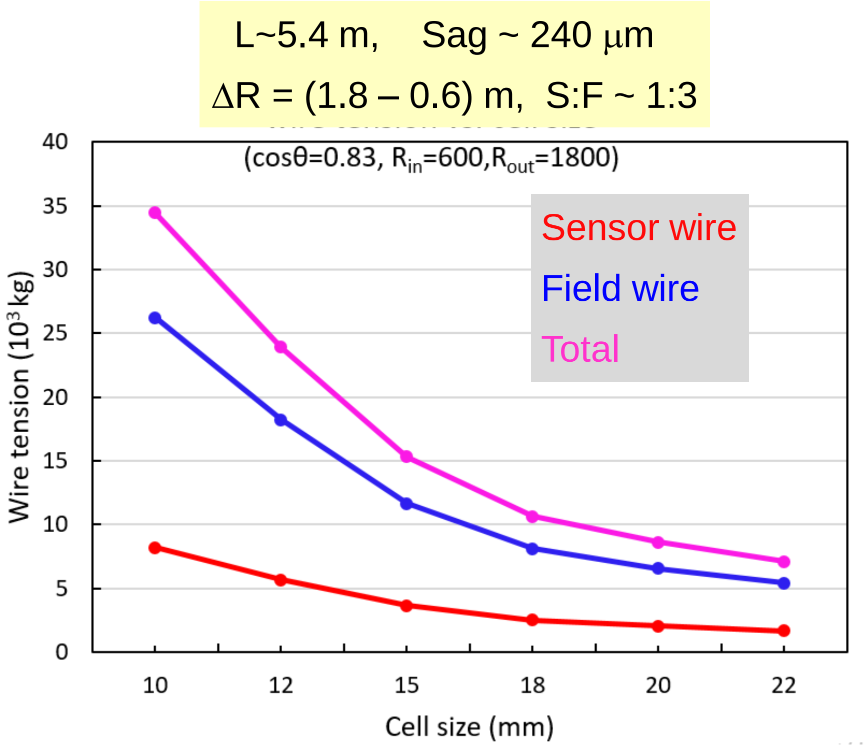

- Increasing the cell size, e.g. x2, has very little effect on the PID performance.
- But it would reduces the number of wires, hence production difficulty, number of readout channels, and material of the supporting structure (mostly at the outer cylinder).
- However, the tracking performance would be worse.

Prototype Test with A Radiation Source

- Prototype test to provide realization parameters for simulation (ongoing)
- Coincidence of scintillator counter trigger provides constraint of incident track angle and track length of electrons from ^{90}Sr source.

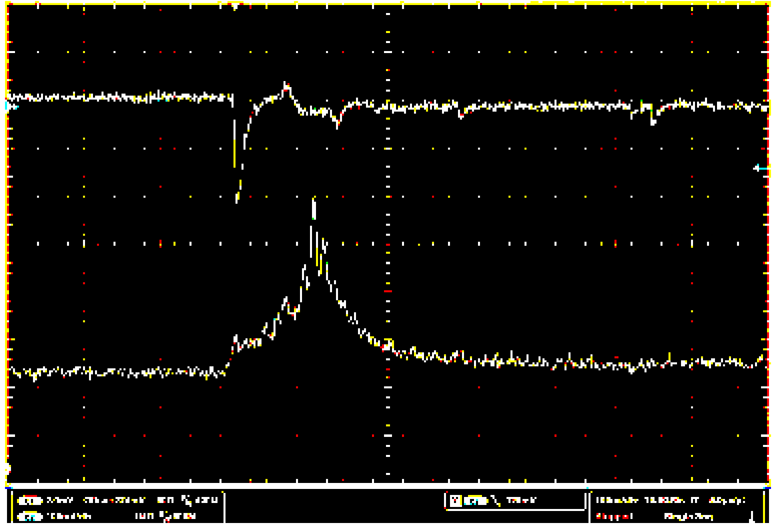

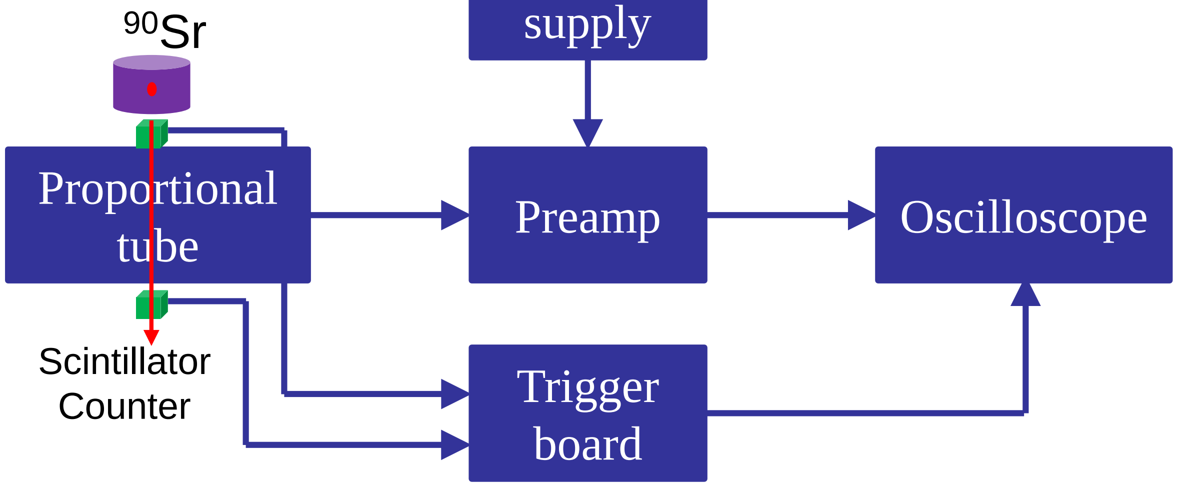

Proportional tube (φ32mm)

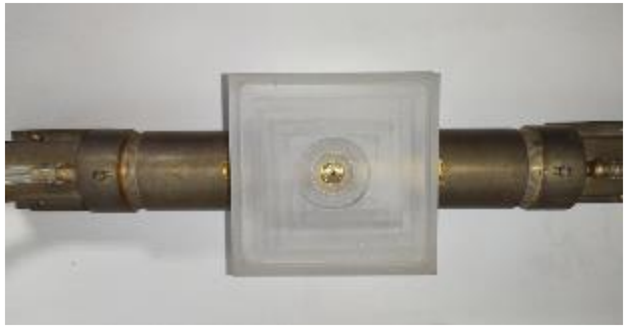

Preamplifier
GBP: 8 GHz

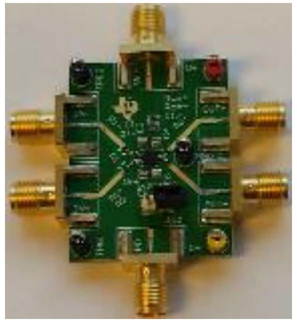

Ongoing Physics Performance Studies

- The criteria of 2σ K/π separation at P<20 GeV is very simplified.
- The drift chamber configuration may also affect the locations of FST layers, and the material before the calorimeters. Thus the impacts on other sub-detectors need to be included in the optimization.
- Ultimately it is the physics reach that decides which configuration is better.
- Benchmark modes were selected for a more meaningful comparison. The studies are on-going with the DC simulation and reconstruction software in progress.

  - $B_s \to (D_s \to KK\pi)\,\pi$
  - $B^0_{(s)} \to hh$
  - $H \to jj$

A Transverse Crystal Bar ECAL That is Compatible with PFA

A PFA Compatible Crystal ECAL

- Calorimetry @ CEPC
  - Precision measurements with Higgs and Z/W
  - Jet energy resolution better than $30\%/\sqrt{E_{\text{jet}}(\text{GeV})}$
  - Particle flow paradigm: high-granularity calorimetry
- Why a crystal ECAL, (instead of Si W)?
  - Even though: larger probability of shower overlap, larger probability of hadronic shower in ECAL comparing to a SiW PFA ECAL
  - Homogeneous structure with EM energy resolution: $\sim 3\%/\sqrt{E} \oplus \sim 1\%$
  - High sensitivity to low energy particles
  - Capability to trigger single photons
  - Precision γ/π^0 reconstruction: flavour and BSM physics
  - Finely segmented crystals: PFA capability for jets.

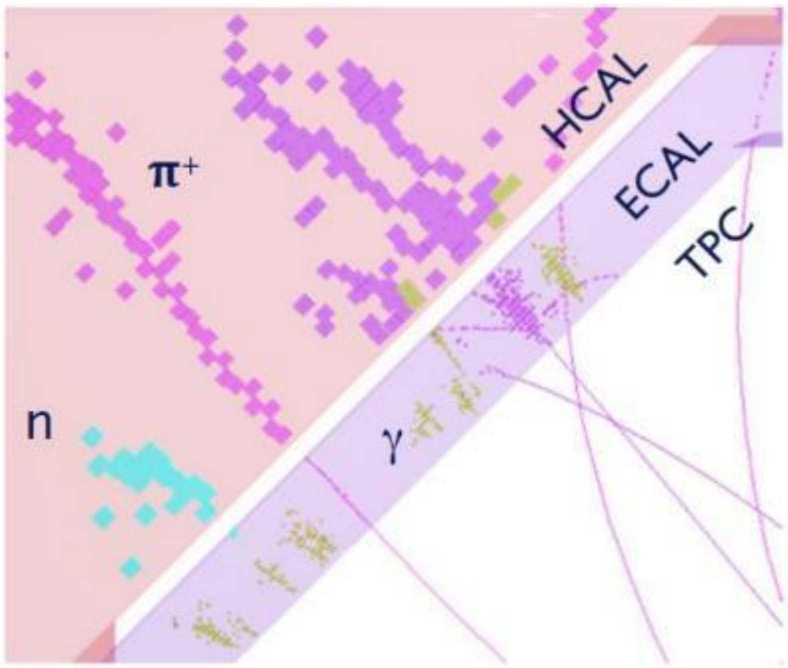

$$\sigma_{Jet} = \sqrt{\sigma^2_{Track} + \sigma^2_{Had} + \sigma^2_{em} + \sigma^2_{Confusion}}$$

Component	Detector	Energy Fraction	Energy Resolution	Jet Energy Resolution
Charged Particles ($X^\pm$)	Tracker	$\sim 0.6\ E_J$	—	—
Photons (γ)	ECAL	$\sim 0.3\ E_J$	$0.15\sqrt{E_\gamma}$	$0.08\sqrt{E_J}$
			$0.03\sqrt{E_\gamma}$	$0.016\sqrt{E_J}$
Neutral Hadrons (h^0)	HCAL	$\sim 0.1\ E_J$	$0.55\sqrt{E_{h^0}}$	$0.17\sqrt{E_J}$

Transverse Crystal Bar ECAL

- A crystal bar ECAL
  - Homogeneous BGO crystal.
  - Bar size ~40×1×1 cm^3, time measurements at two ends for position along the bar.
  - Crossed arrangement in adjacent layers. Two layers form a super cell module: ~40×40×2 cm^3.
  - Reduce readout channels, minimize dead materials.

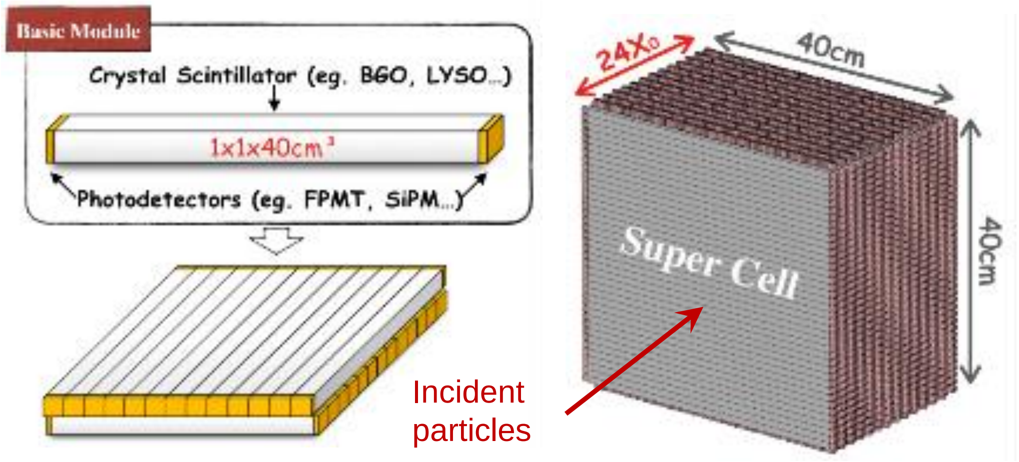

- Key issues:
  - Ambiguity caused by 2D measurements (**ghost hit**).
  - Identification of energy deposits from individual particles (**confusion**).

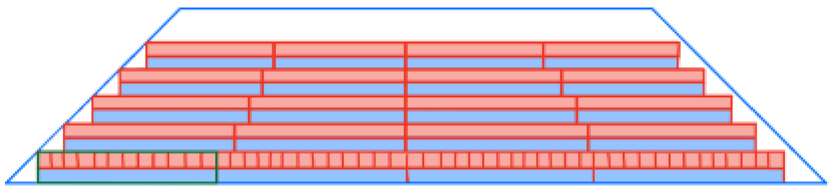

- Ongoing work:
  - Use ArborPFA software & crystal cubes of 1 cm^3 in size to study PFA performance, compare with SiW ECAL.
  - Develop a proto-PFA new software that has separation capability of multiple incident particles.
  - Bench test of crystal bars.

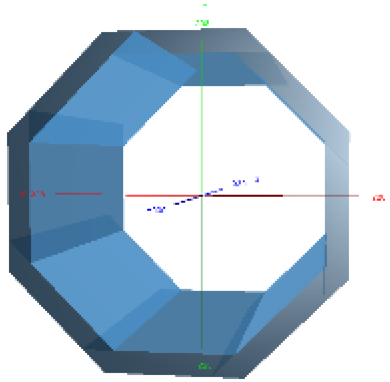

8 trapezoidal staves

R=1.8m, L=4.6m, H=28cm

Separation Power of Two Photons

Two 5 GeV γ's

Sketch of ECAL in r-z plane

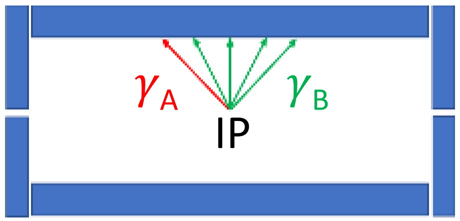

- Two gammas (5GeV): varying distance
- Efficiency definition: successful reconstruction of **at least 2 neutral particles, both in 3.3GeV<E<6.6GeV**
- Removed events with γ-conversion before entering ECAL
- Applied energy calibration

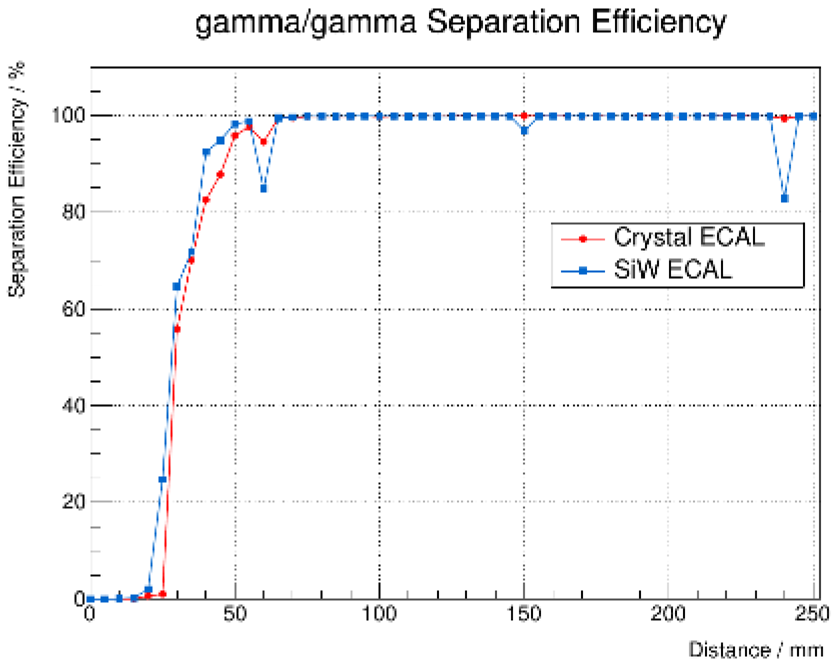

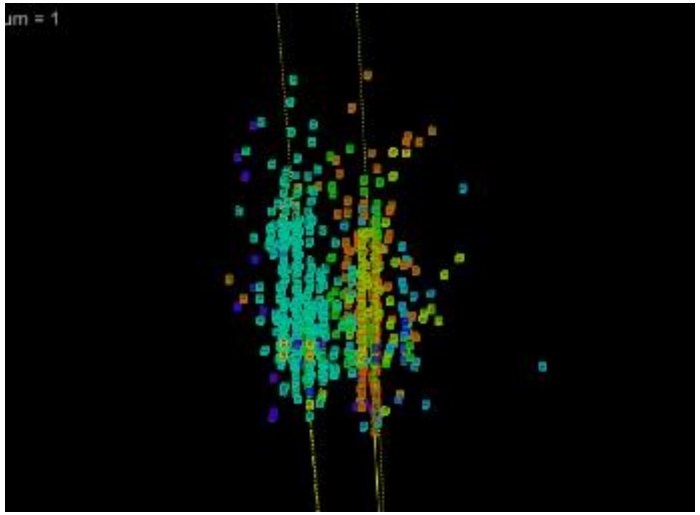

Crystal: distance 50 mm successfully reconstructed

- Similar separation performance achieved in two ECAL options: crystal and SiW
- Next step: try to apply shower profile information (benefits of fine segmentation)

Separation Power of $\pi^+\gamma$

10GeV π^+ and 5GeV γ

Separation of a gamma and a charged pion

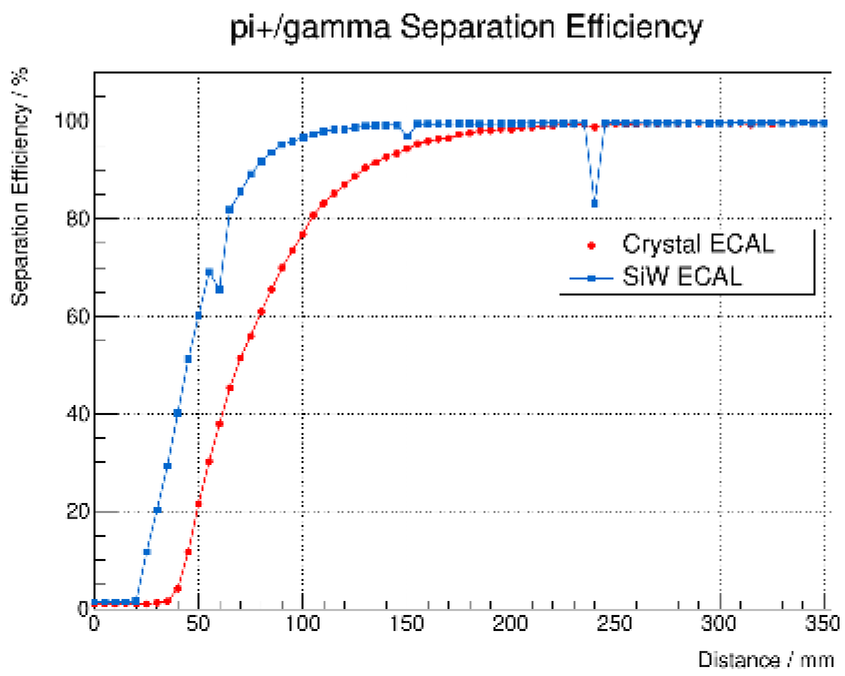

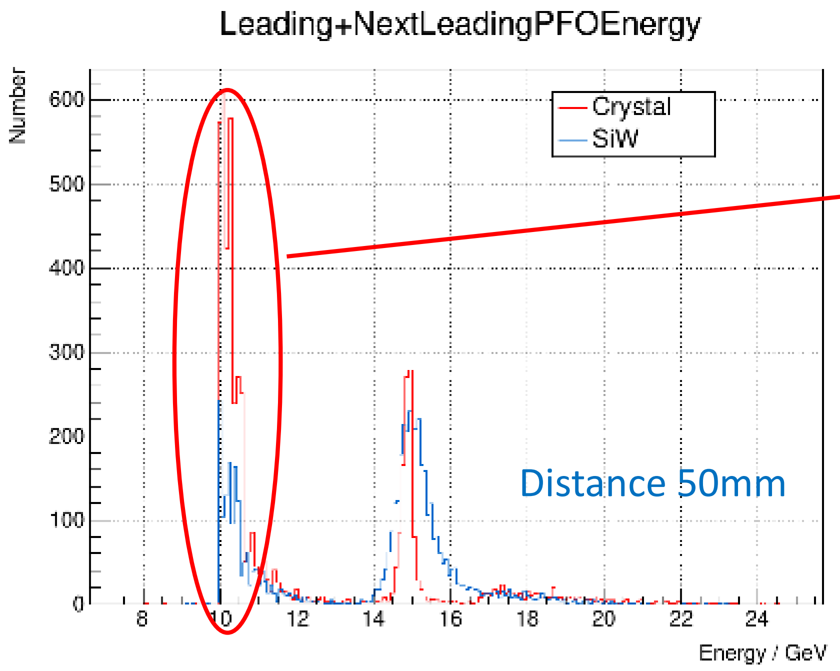

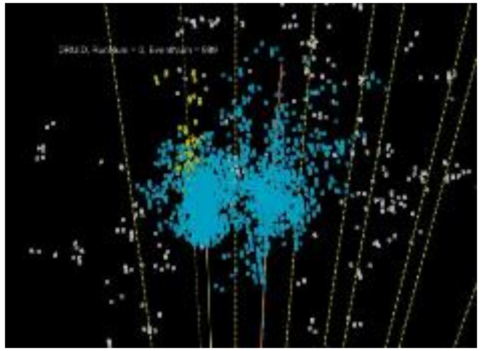

Failure in track-calo matching: cluster of photon (left) was wrongly absorbed into the cluster of π^+ (right), the energy of photon would be lost

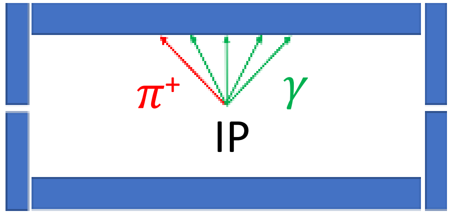

- 10GeV π^+ and 5GeV γ: varying distance
- 3 T magnetic field
- π^+ momentum measured by tracker
- Efficiency definition: successful reconstruction of **3.3GeV<E_N<6.6GeV, 9.9GeV<E_C<10.1GeV**
- Removed events with γ/π^+ interactions before entering ECAL
- Applied energy calibration

- Next step: try to apply shower profile information (benefits of fine segmentation)

Neutral Pion Reconstruction with Arbor-PFA

Single 7 GeV π^0's generated by the particle gun

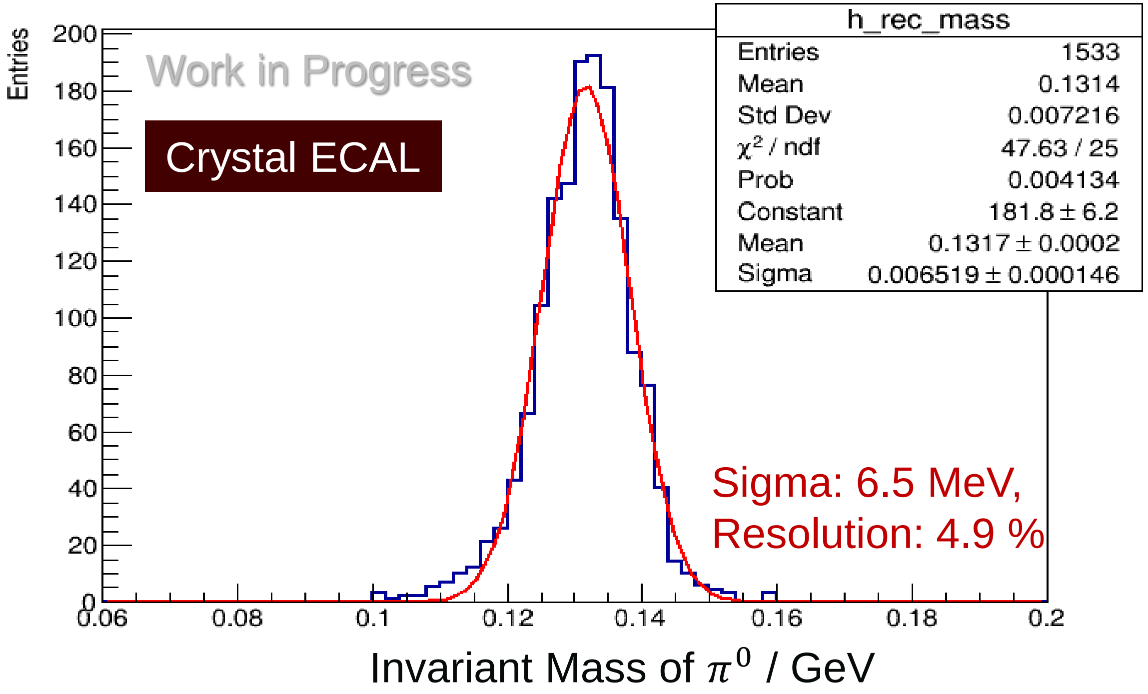

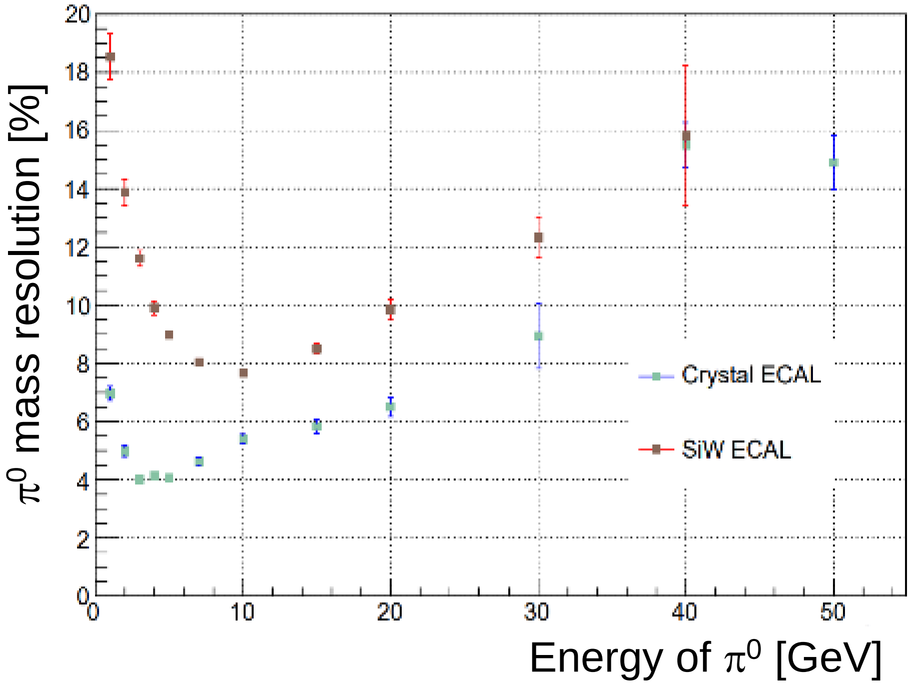

Crystals show optimal performance in general, especially at a few GeV

Physics Benchmark: $H \rightarrow \gamma\gamma$

- Full simulation studies with $ZH(Z \rightarrow \nu\nu, H \rightarrow \gamma\gamma)$ at 240 GeV
  - Promising BMR (Boson Mass Resolution)
  - Identified impacts of the geometry boundaries

Structures around the Higgs invariant mass peak

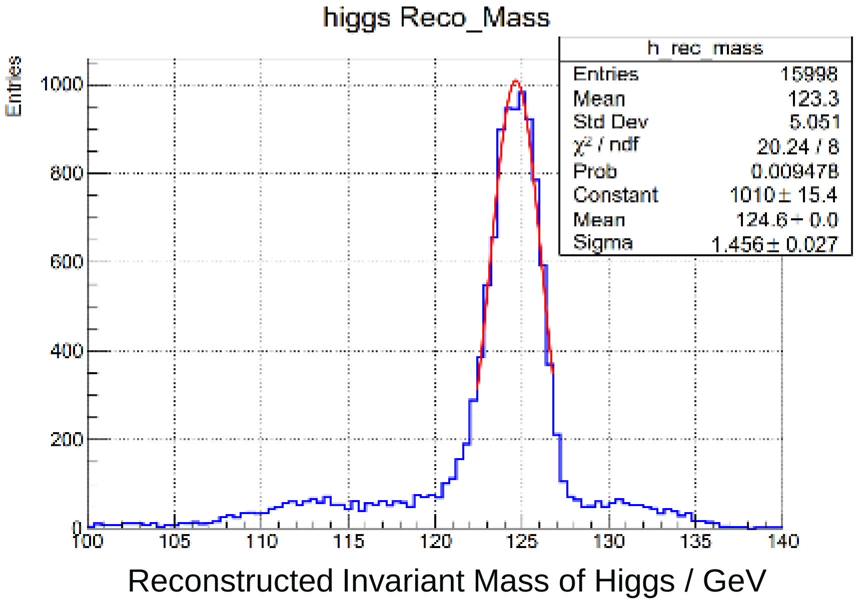

Gaps in the barrel ECAL (octaves)

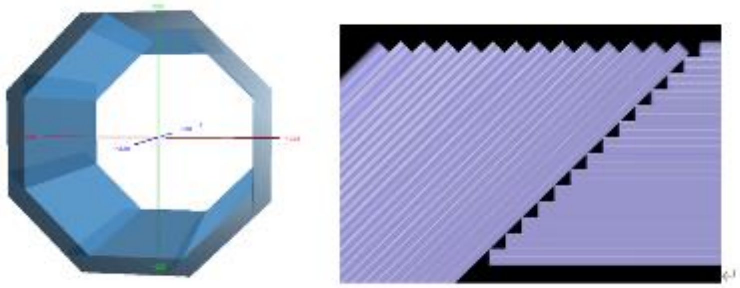

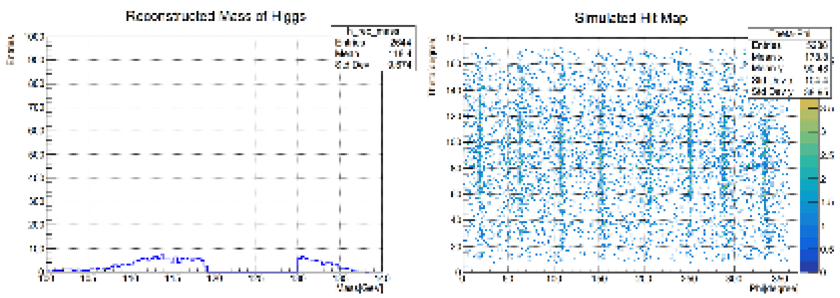

BMR of SiW ~ 2.3%

Excluding hits near gaps

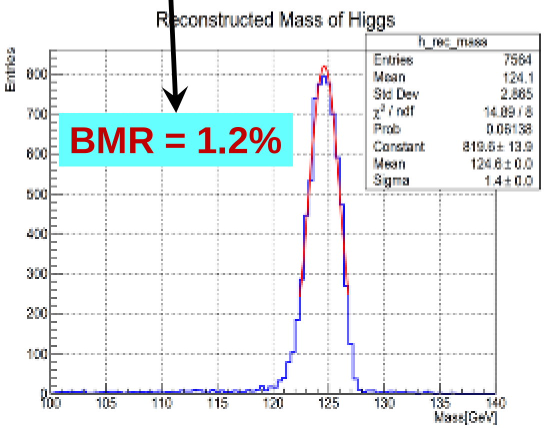

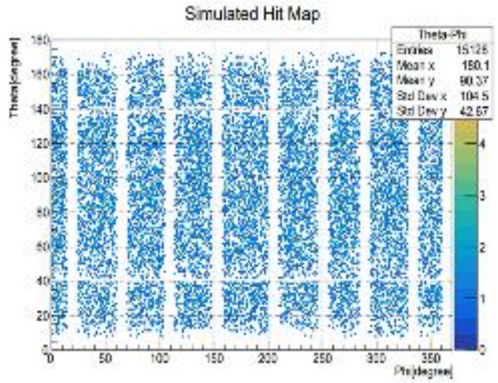

Physics Benchmark: $H \to gg$

- Physics benchmark: $ZH(Z \to \nu\nu, H \to gg)$ at 240 GeV
- Potentials to be explored with more information: e.g. shower profile, timing, etc.

SiW ECAL

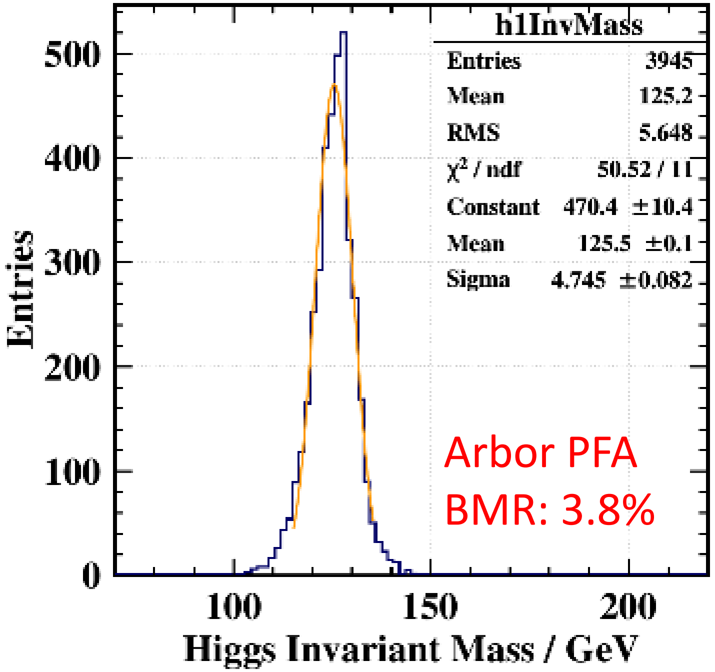

Crystal ECAL

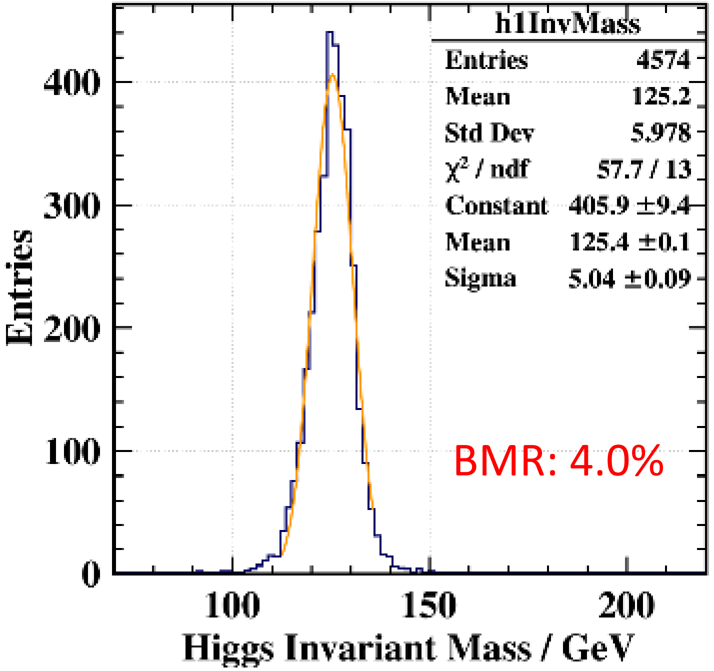

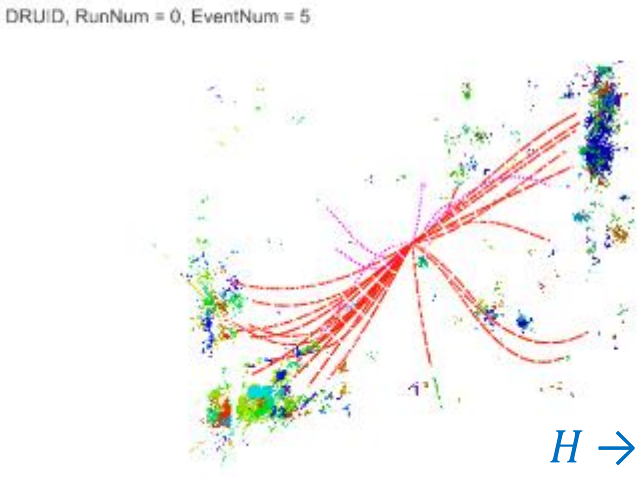

$H \to gg$

A New Proto-PFA Software

No track-calo matching, fragment absorption, etc

- 1 Dimension
  - Clustering and energy splitting
- 2 Dimension
  - Matching energy and time measurements in adjacent layers
- 3 Dimension
  - Cone clustering longitudinally.

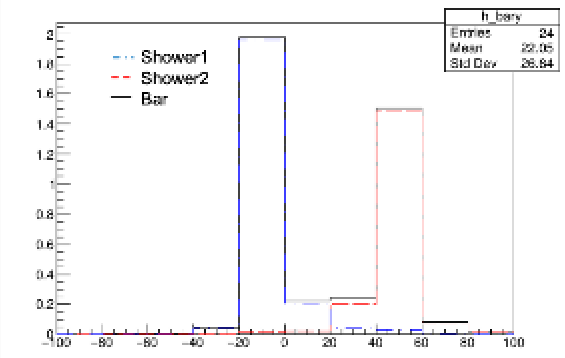

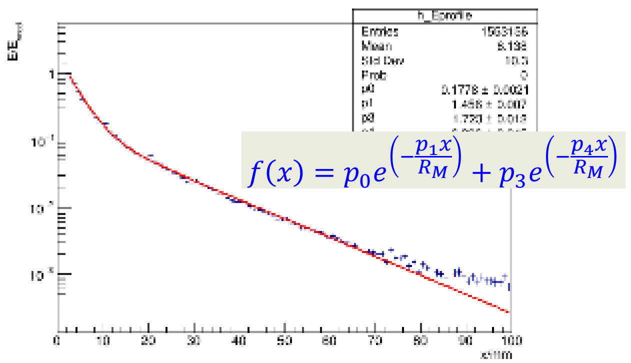

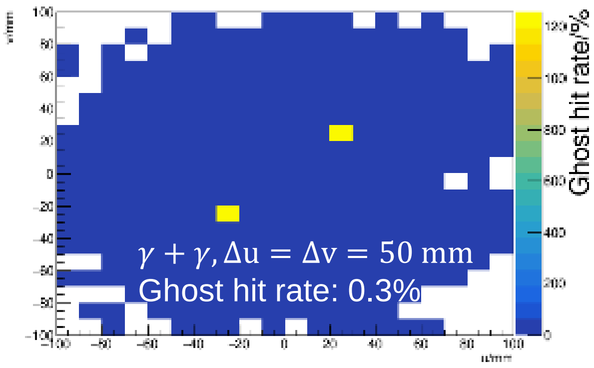

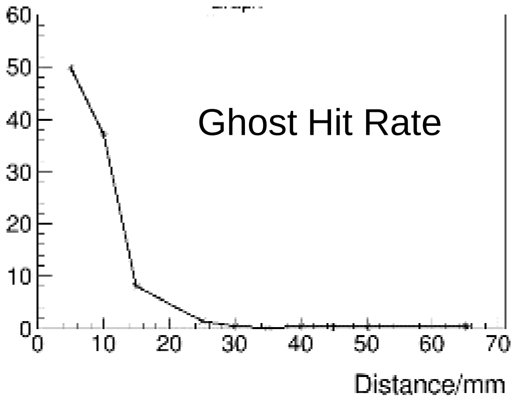

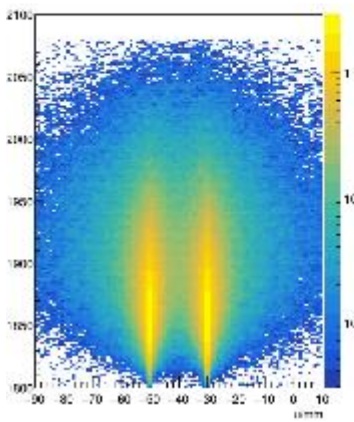

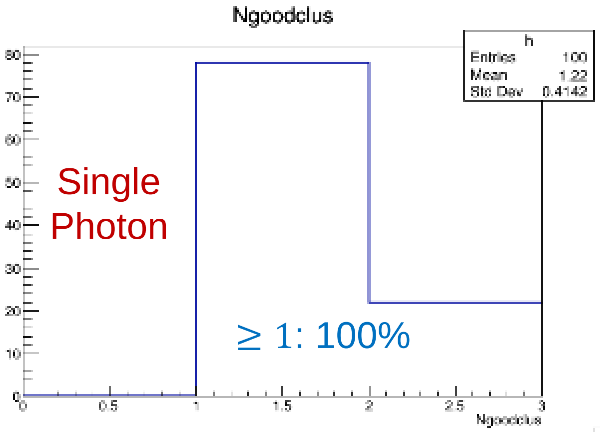

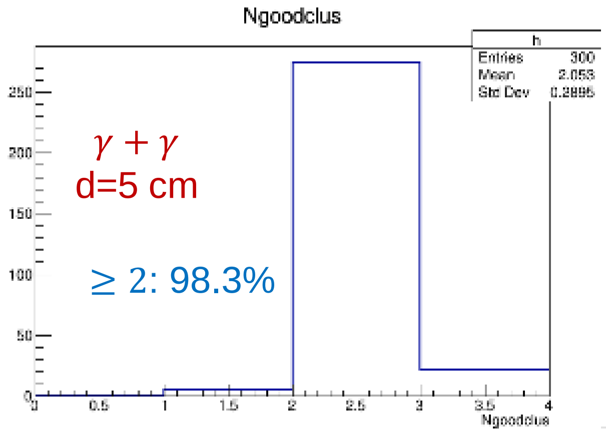

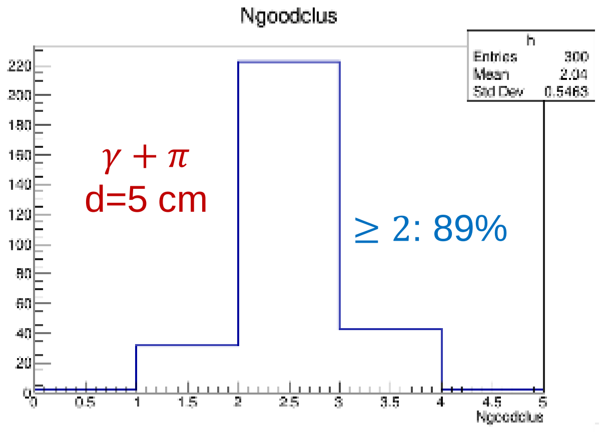

Performance of The New Software

Separation power of two 5 GeV γ's in parallel

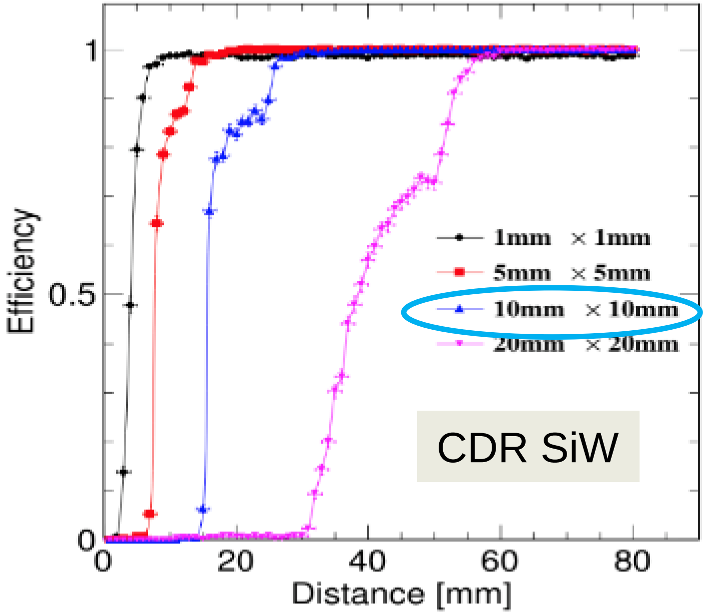

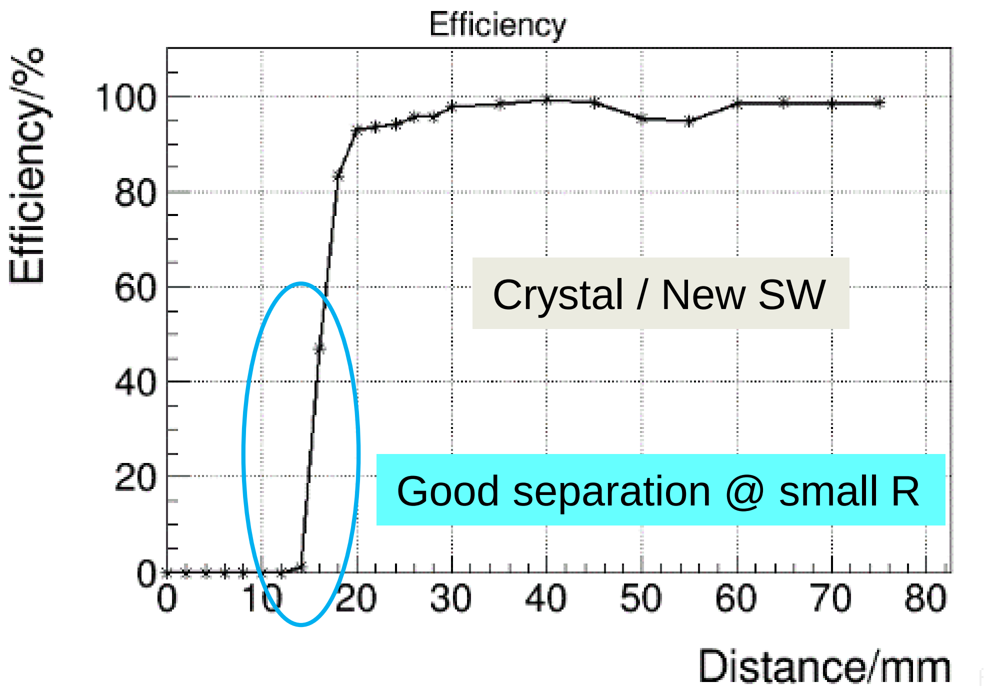

"Proto-PFA" Development for Long Bars

- Developing a new PFA software for crystal ECAL:
  - Traditional PFA: fine granularity + small R_M + less hits (sampling) for separation.
  - Crystal PFA: precise energy (homogeneous) + shower profile for separation.

- χ^2 method for ghost hit removal is very efficient. ➔ Ghost hit problem ✓
- Energy splitting shows potential for particle separation. ➔ Confusion ✓
- Preliminary result is promising.

- Many details still need optimization:
  - Clustering efficiency,
  - Fragment absorption (cluster merging),
  - Cluster ID efficiency & mis-ID rate,
  - ……

Uniformity Scan in Geant4 Simulation

Geant4 10.7

- 40×1×1 cm^3 long BGO crystal bar
- 662 keV gamma from Cs-137
- Varying Cs-137 positions

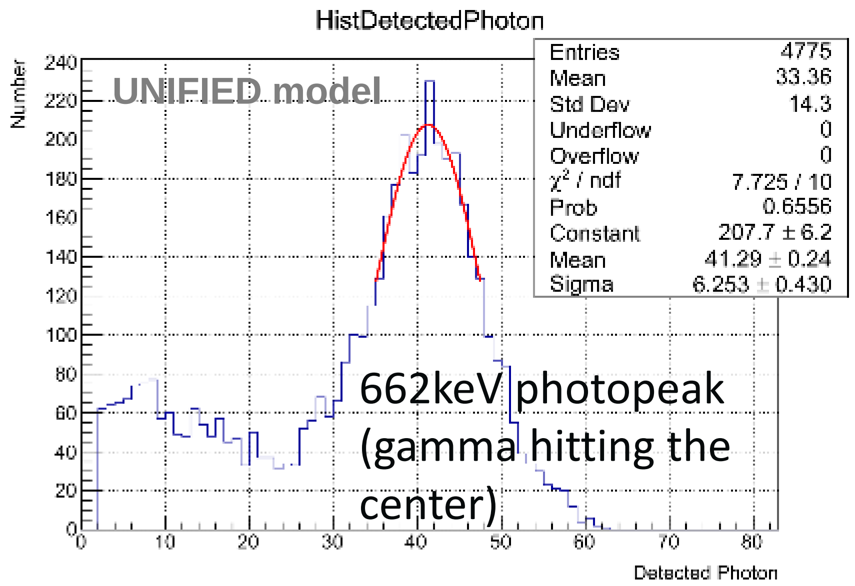

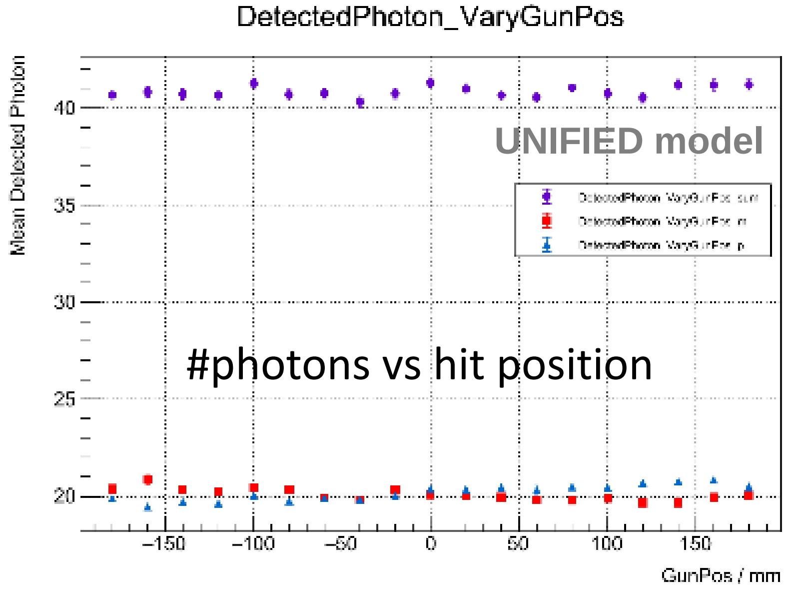

- Generally good response uniformity expected in G4 simulation

First Measurements of The Uniformity Scan

- Setup: 400mm long BGO crystal (with ESR foil) and ^{137}Cs source
- The same configuration as the simulation

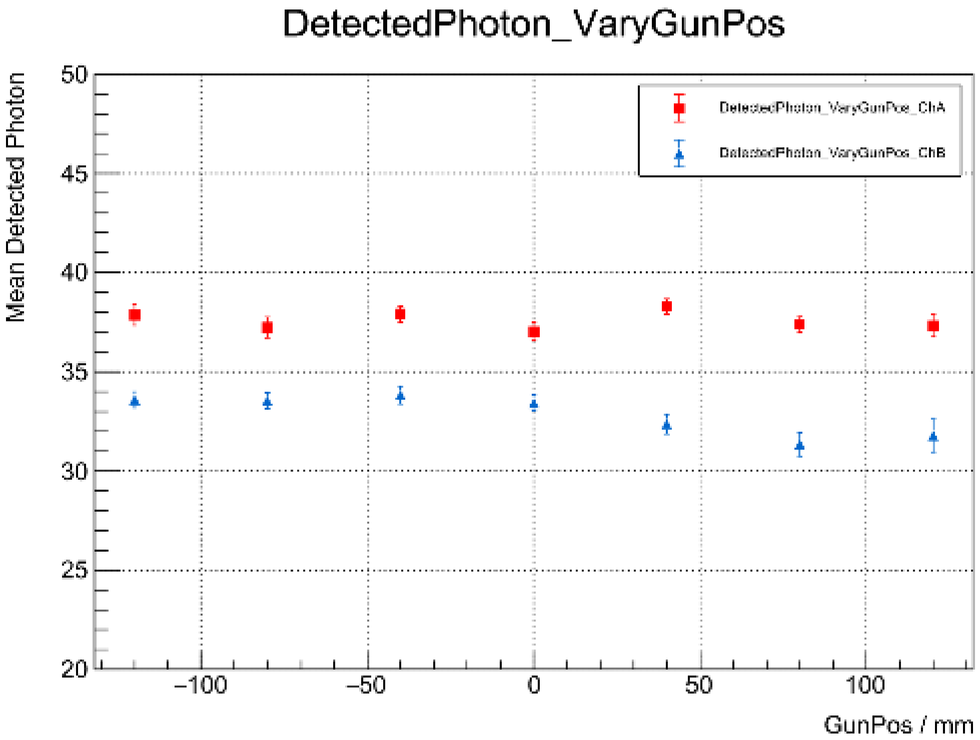

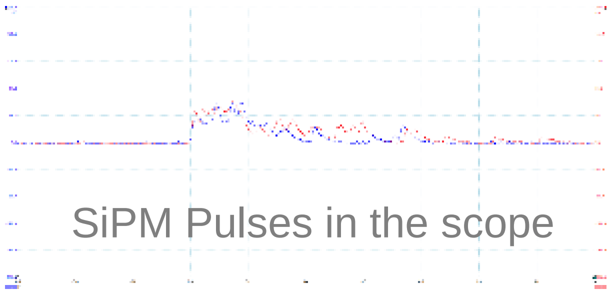

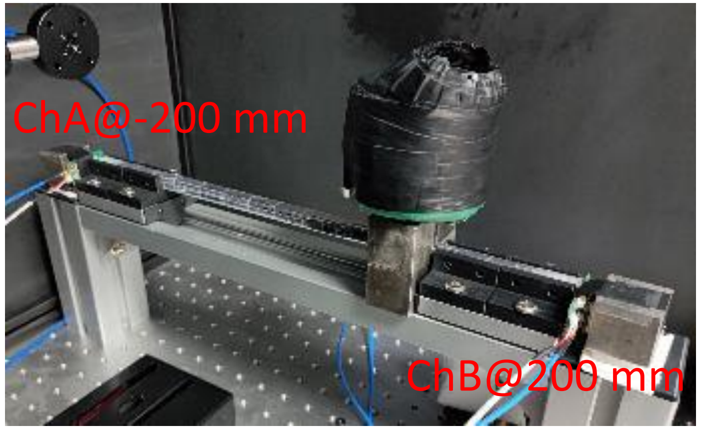

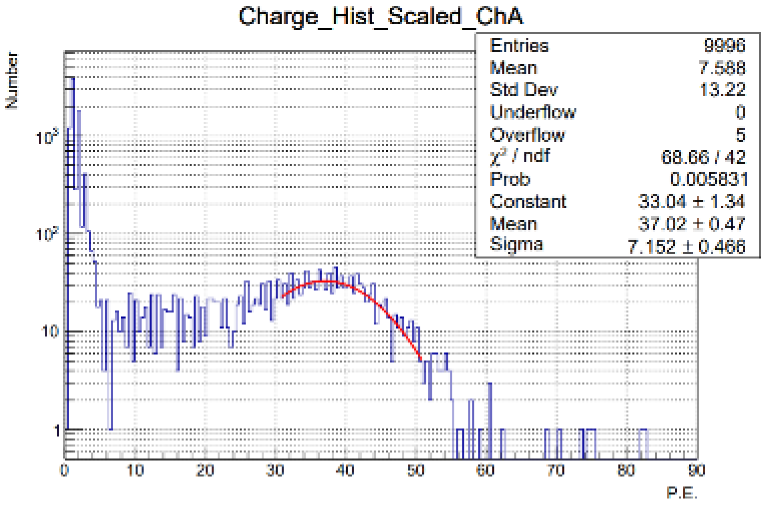

- Trends are not significant enough due to the systematic difference between 2 SiPMs
- Refractive indices of materials
    - Air: 1.00
    - Epoxy: 1.52
    - BGO: 2.15

- Ongoing activities: to use optical grease to improve the crystal-SiPM coupling and reproducibility

Impacts of Wrapping and Surfaces

- ESR foil wrapping and polished surface show better energy resolution

$2 \times 2 \times 8\ \mathrm{cm}^3$ BGO bar

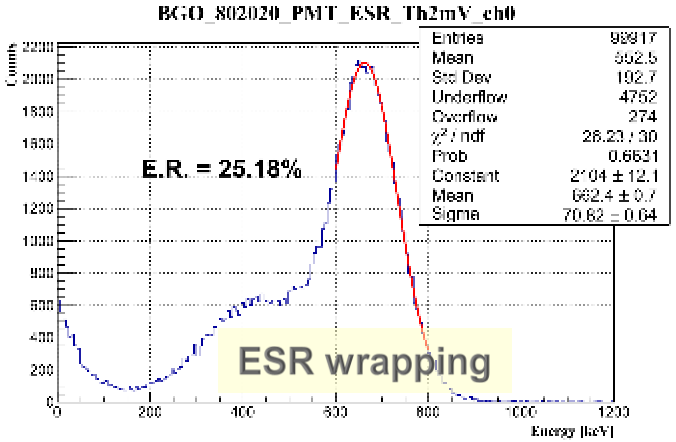

$1 \times 1 \times 8\ \mathrm{cm}^3$ BGO bar

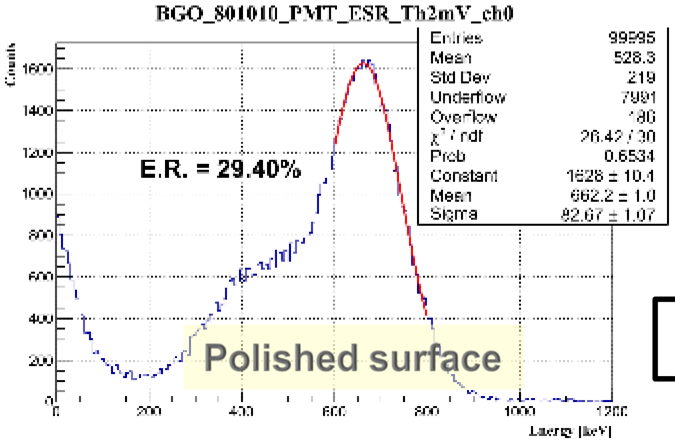

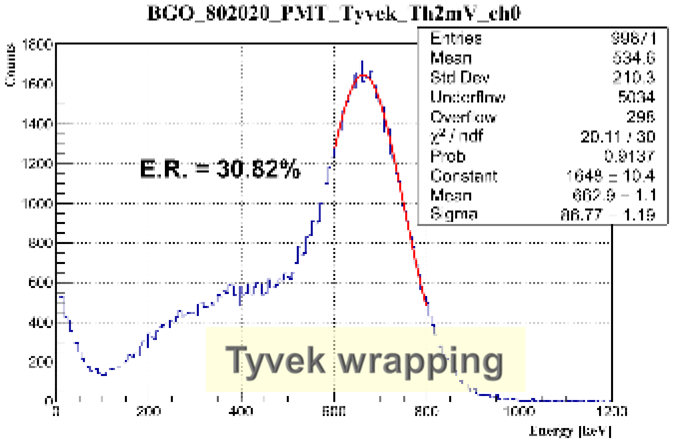

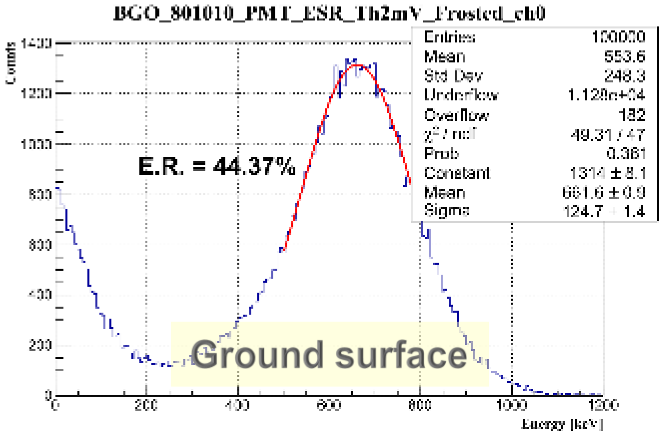

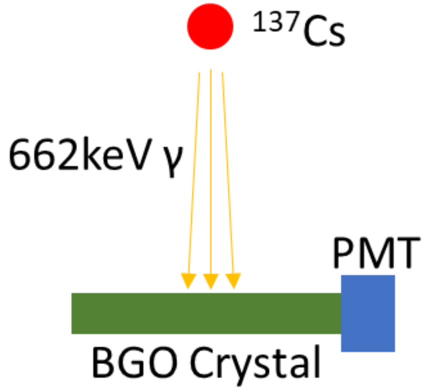

Energy Resolution (E.R.) = $2.355 \times \frac{\sigma}{mean}$, defined as FWHM

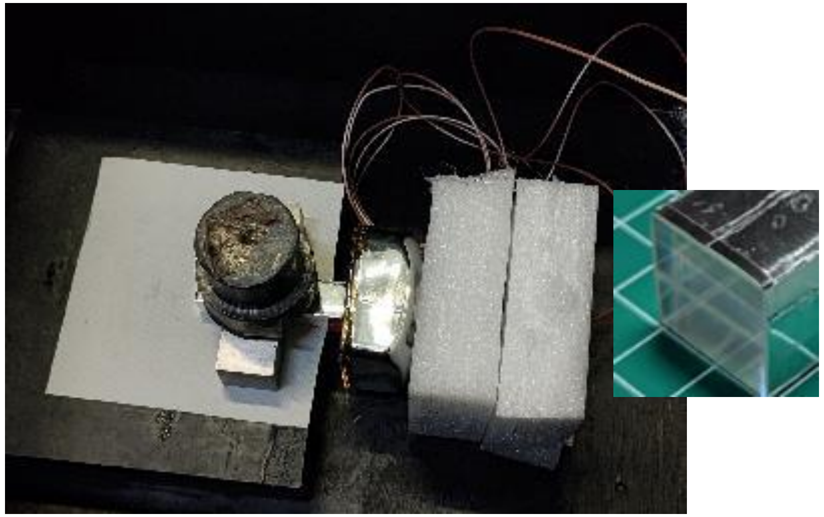

Impacts of Crystal Length

PMT

SiPM

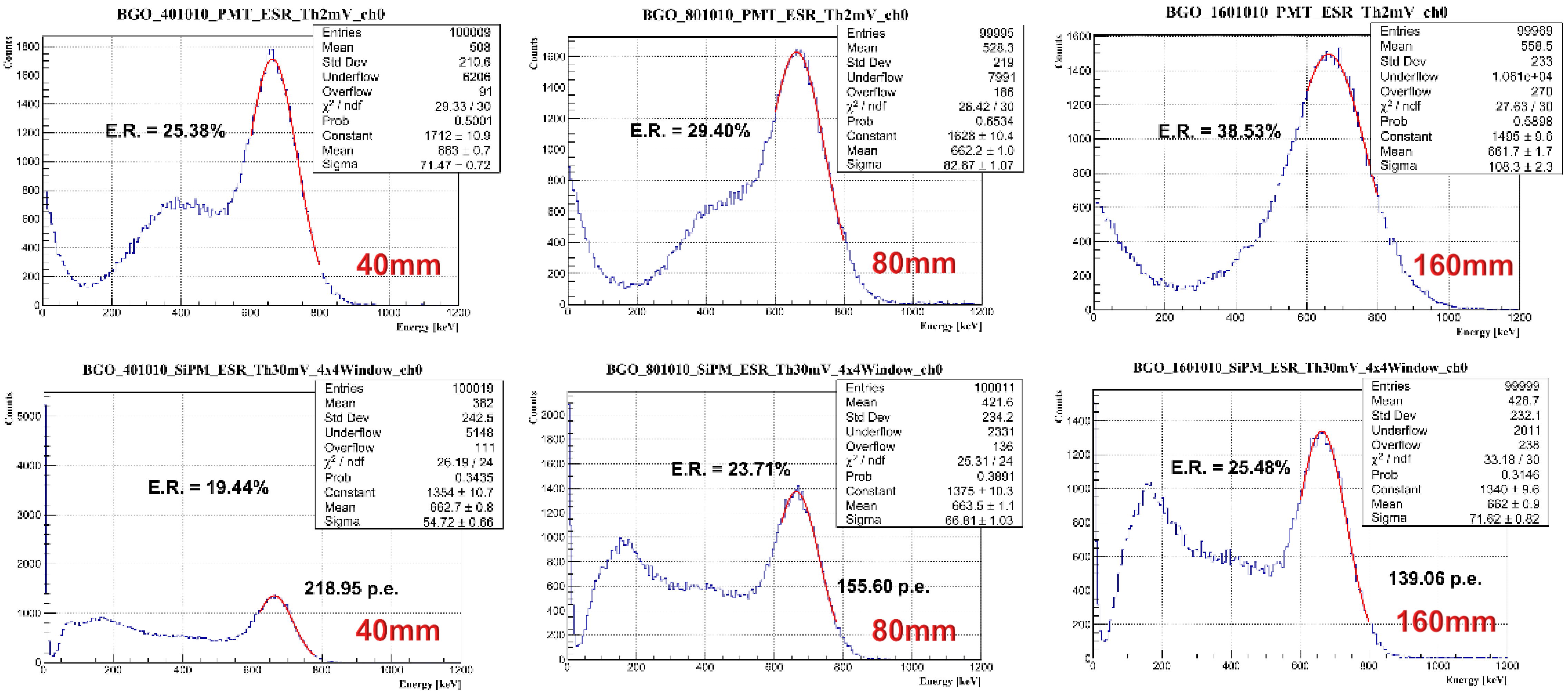

- PMT has better acceptance (full coverage of crystal transverse area) than SiPM; to be updated with larger SiPMs
- Further comparisons will be done with simulation

A PFA HCAL
Based on Scintillation Glass

A HCAL Based on Scintillation Glass

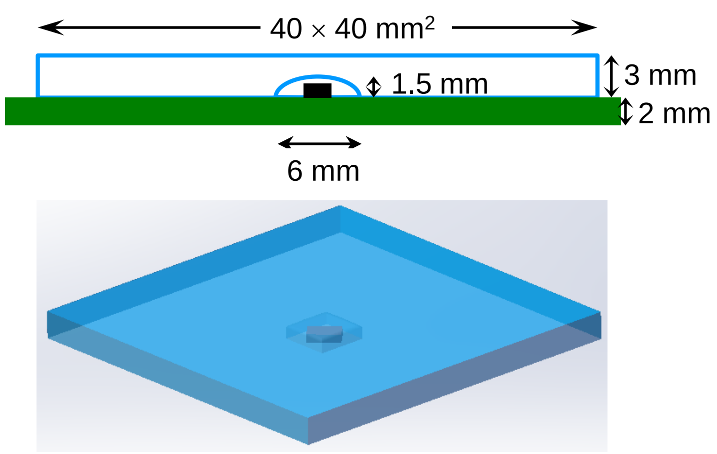

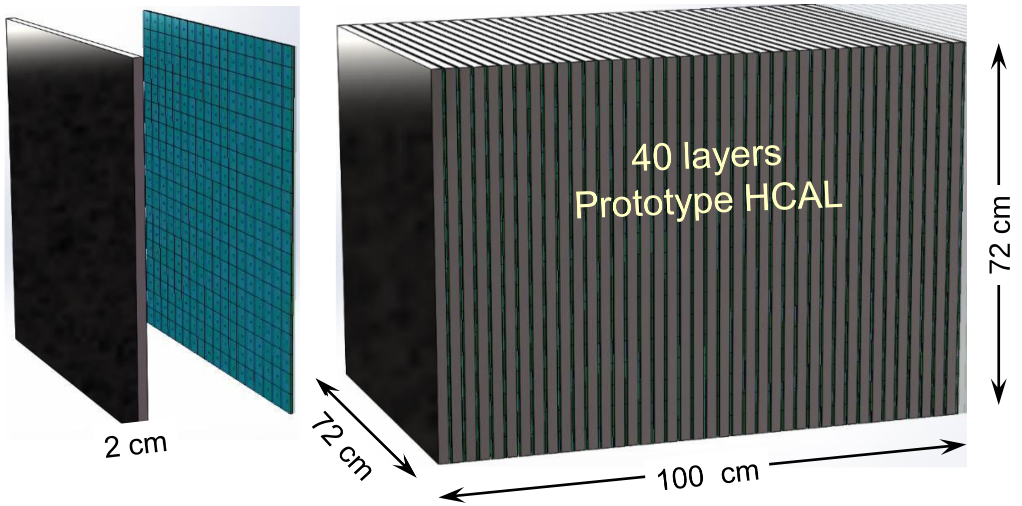

- On-going R&D of a HCAL of steel + plastic scintillator + SiPM.
- The plastic scintillator can be replaced with scintillation glass, e.g. those in the table.

Sample nos.	Molar compositions	Density (g/cm^3)	Radiation length (cm)	Integrated light yield (% of BGO)
S0	$20SiO_2–35B_2O_3–15BaF_2–15Lu_2O_3–15Gd_2O_3$	5.6	–	–
S1	$20SiO_2–38B_2O_3–15BaF_2–15Lu_2O_3–10Gd_2O_3–2CeF_3$	5.2	1.81	54
S2	$20SiO_2–33B_2O_3–15BaF_2–15Lu_2O_3–15Gd_2O_3–2CeF_3$	5.6	1.67	87
S3	$20SiO_2–28B_2O_3–15BaF_2–15Lu_2O_3–20Gd_2O_3–2CeF_3$	6.0	1.56	58
S4	$20SiO_2–38B_2O_3–15BaF_2–10Lu_2O_3–15Gd_2O_3–2CeF_3$	5.1	1.89	81
S5	$20SiO_2–28B_2O_3–15BaF_2–20Lu_2O_3–15Gd_2O_3–2CeF_3$	6.2	1.48	86

Wang, Qian, et al. "High light yield Ce3+-doped dense scintillating glasses." *Journal of alloys and compounds* 581 (2013): 801-804.

Energy Resolution From Simulation

Varying thickness of Steel

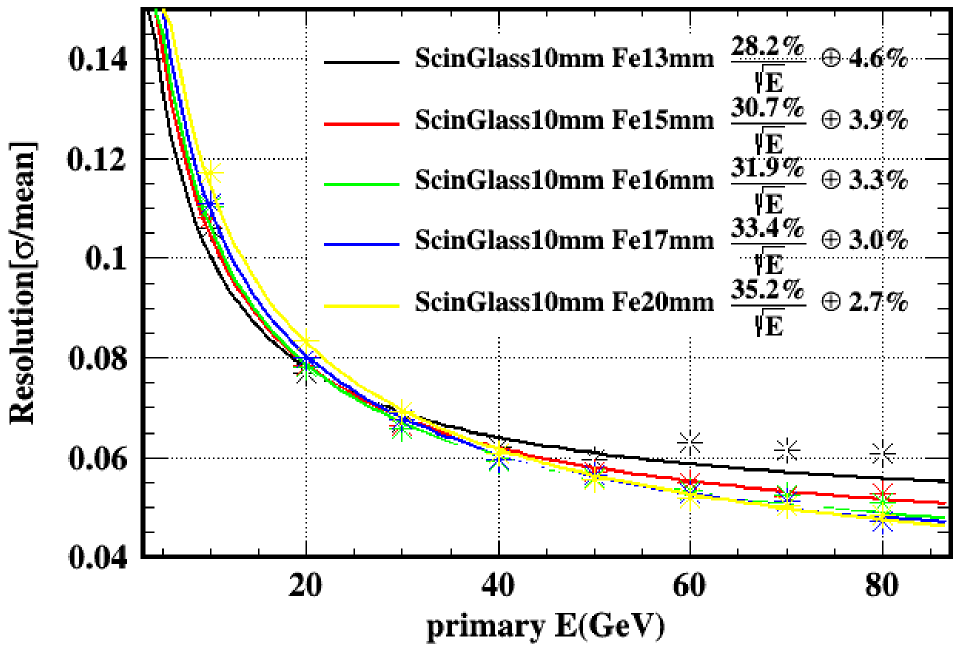

Varying thickness of ScintGlass

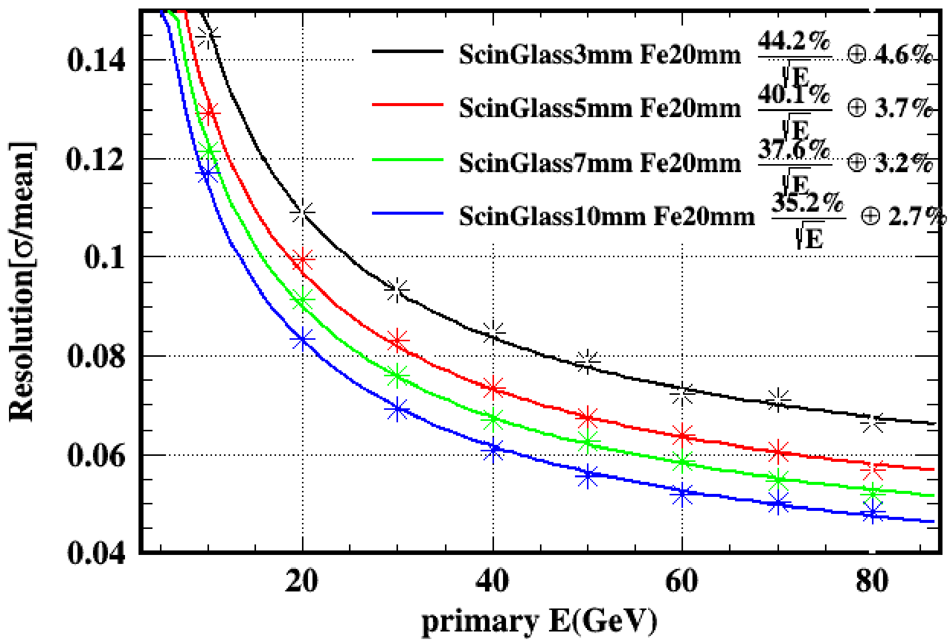

Simulation study of K_L particle gun on a Scintillation Glass HCAL.

ScintGlass: ρ=5.1 g/cm^3, X_0=1.89 cm, light yield = 81% of BGO

HCAL of ScintGlass vs Plastic Scintillator

- With CEPC geometry including HCAL of cell size 40x40 mm^2
- 3mm plastic scint + 20mm Fe vs 6mm scint glass + 17mm Fe

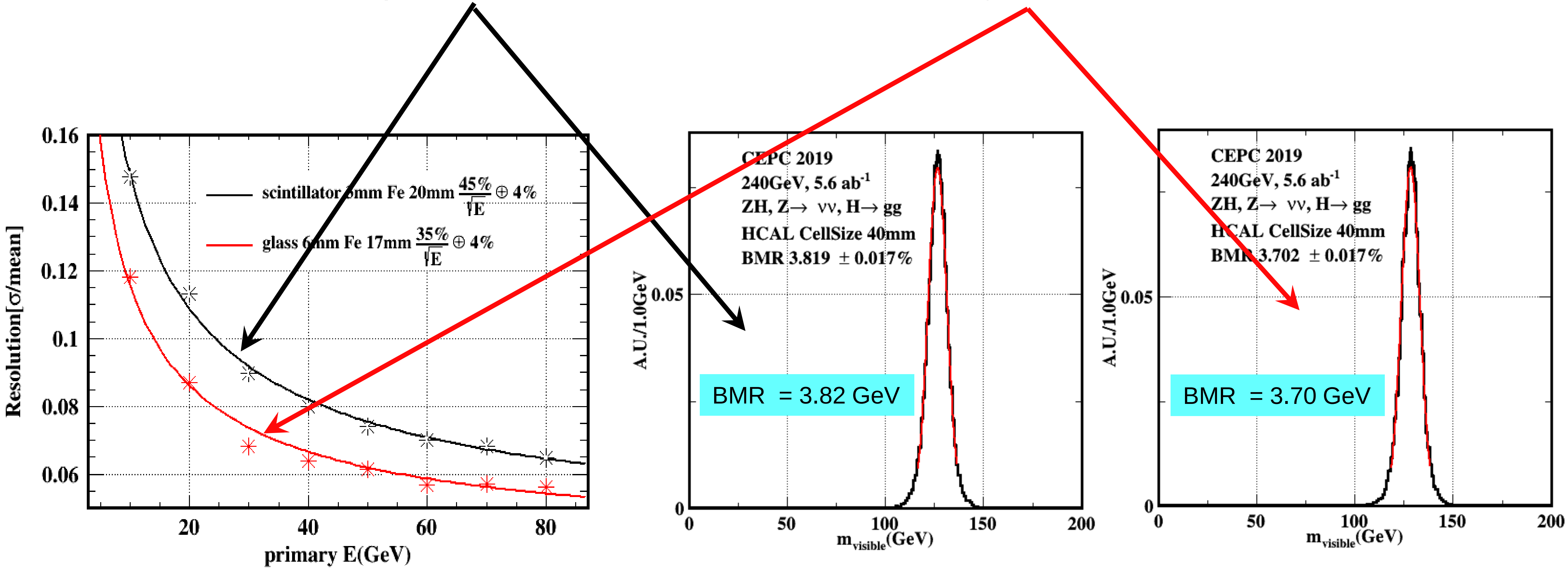

Lab Setups To Study ScintGlass

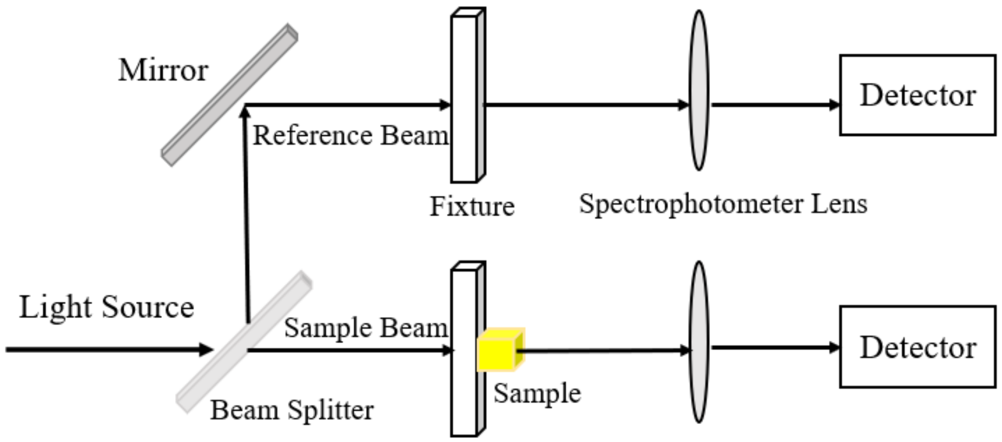

Transmission Spectrum Measurement

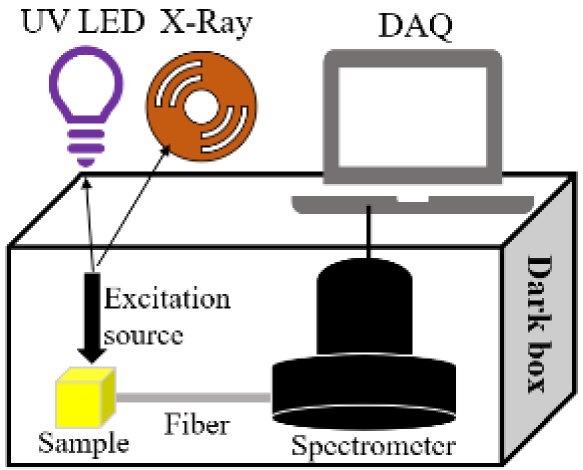

Emission Spectrum Measurement

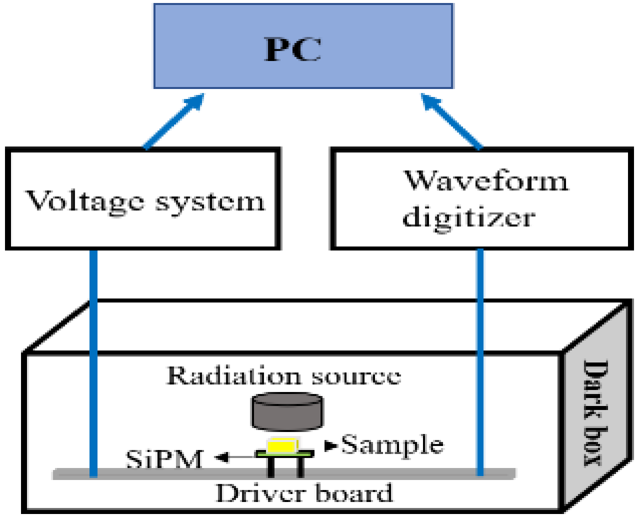

Energy resolution Measurement

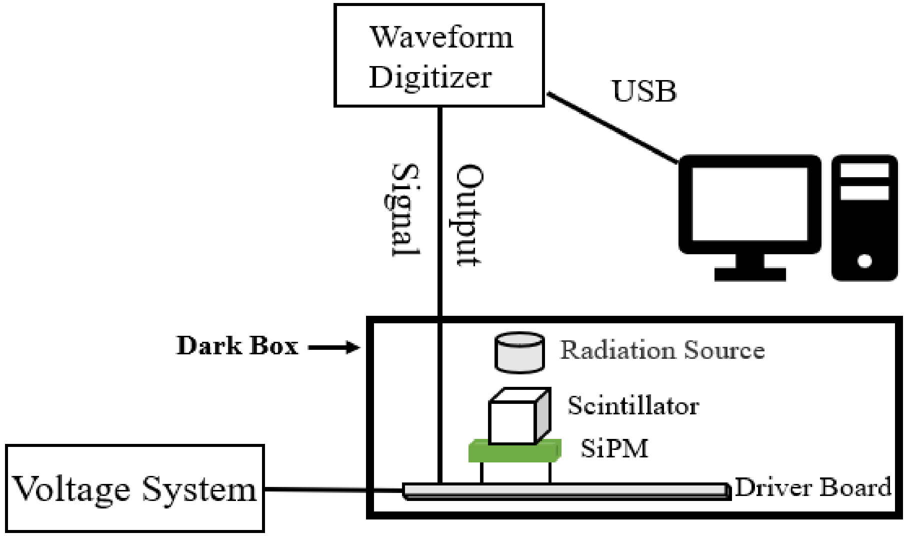

Light Yield Measurement

Samples of Scintillation Glass

Sample from JGSU

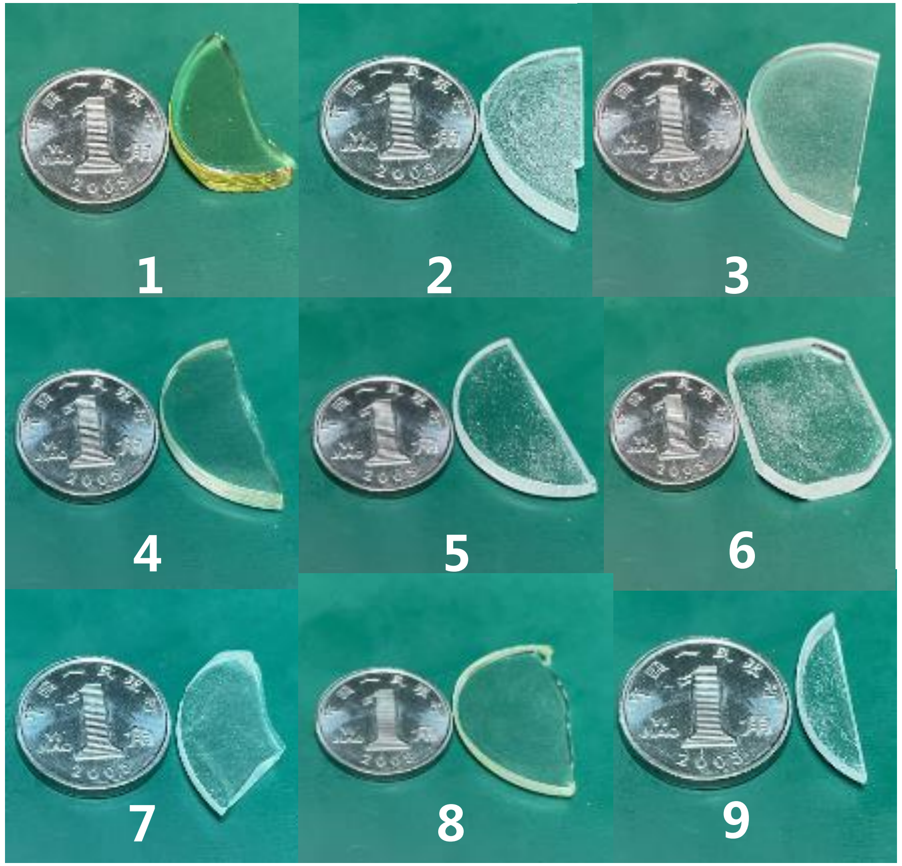

Sample from CBMA

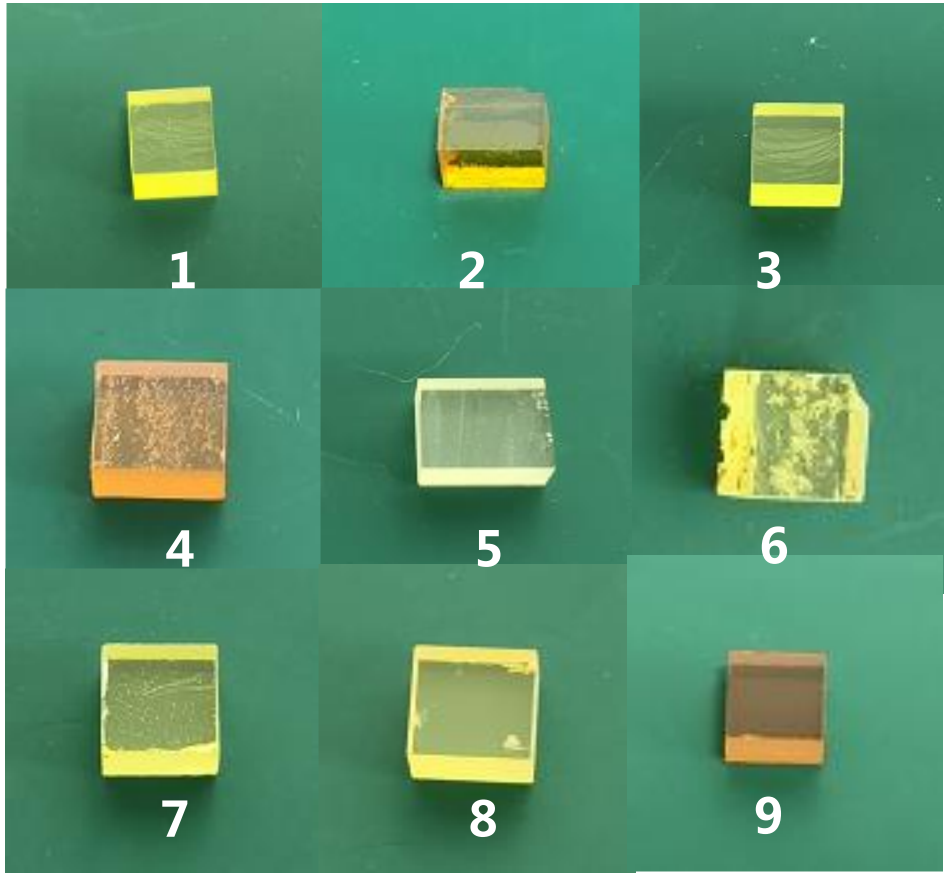

A small collaboration may be formed soon to study scintillation glasses and share information.

Quick Test Results of Samples

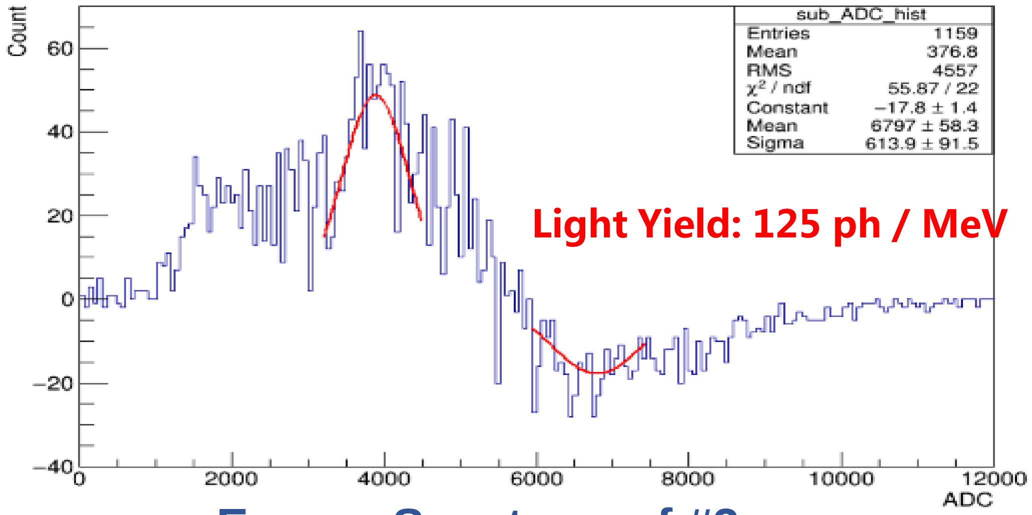

Energy Spectrum of #2

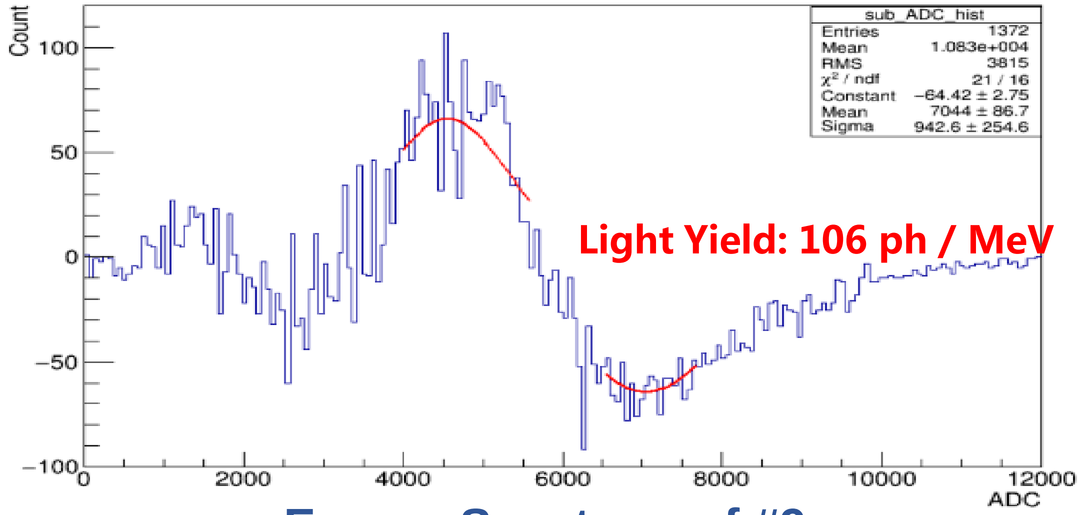

Energy Spectrum of #9

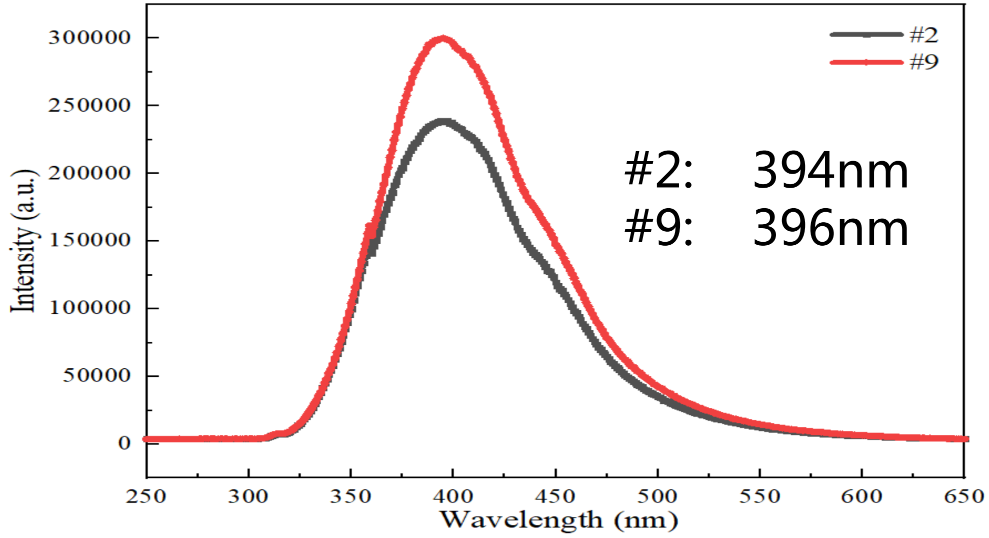

Emission spectra of X-ray induced

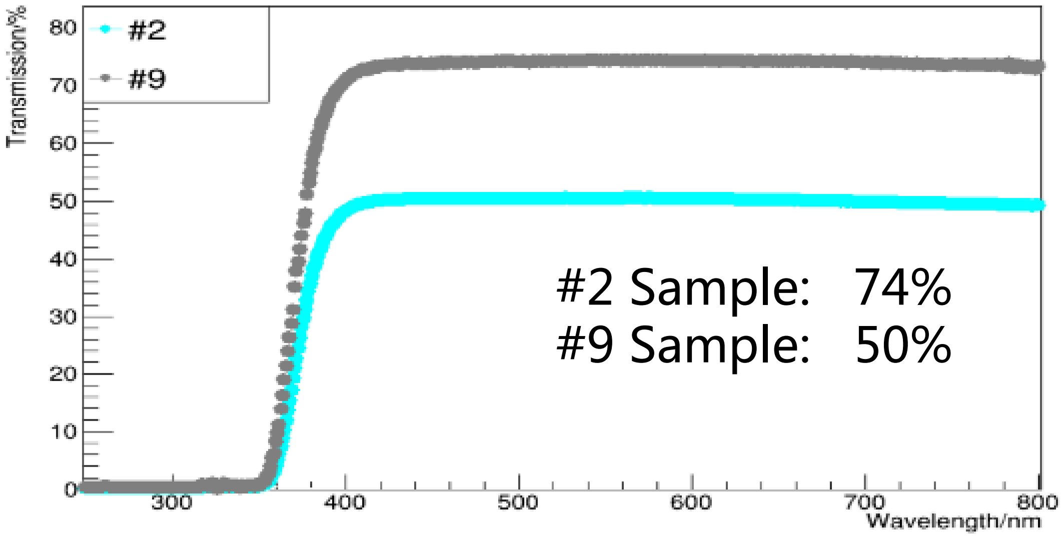

Transmission Spectrum

Performance Comparison & Goal

Typy	Composition	Density (g/cm^3)	Light yield (ph/MeV)	Decay time (ns)	Emission peak(nm)
Scintillator Glass In Paper	Ce-doped high silica glass	4.37	3460	522	431
	Ce-doped gadolinium borosilicate glass	4.94	1120	29.3	394
	Ce-doped fluoride glass	6.0	2400	23.4	348
Plastic Scintillator	BC408	~1.0	5120 ?	2.1	425
	BC418	~1.0	5360 ?	1.4	391
Crystal	GAGG:Ce	6.6	50000	50.1	560
	LYSO:Ce	7.3	25000	40	420
Scintillator Glass for CEPC	?	**>7**	**>1000**	50	350-500
Scintillator Glass Sample in Lab	Ce-doped-Gd-glass	~4.5	~120	~400	400
	Ce-doped-Si-Ba-glass	~5.0	~70	~170	500-550

A HTS Magnet
To Be Placed Inside HCAL

Solenoid Magnet Inside HCAL

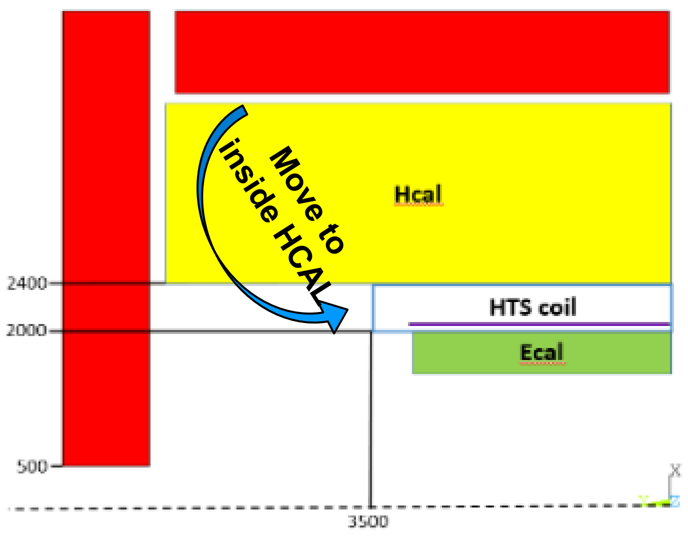

Challenges

Low mass, ultra-thin, high strength cable

- Inner radius = 2.33m, length < 8m, central magnetic field: 3 T
- Magnet radial thickness < 150 mm
- Mass of magnet < $1.5X_0$

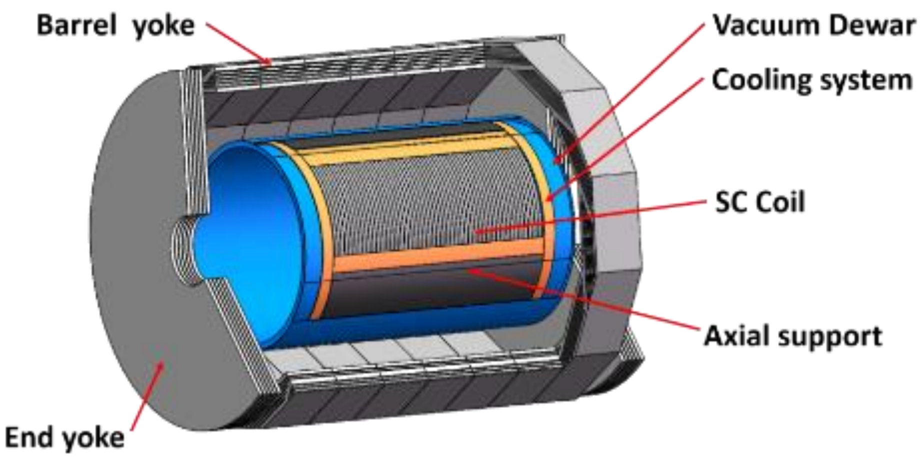

R&D: high strength HTS cable, ultra-thin cryostat.

Al stabilized ReBCO stacked tape cable

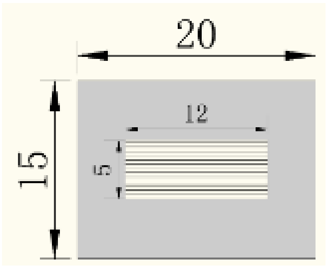

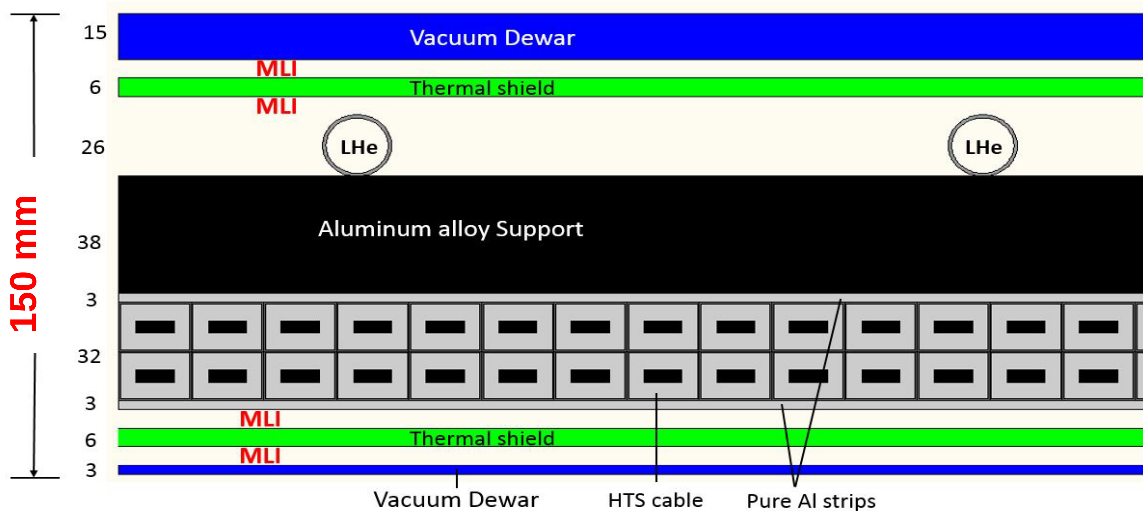

HTS cable length (km)	9
ASTC weight(ton)	9
Operating current(A)	29700
Cold mass weight (ton)	20
Total weight (ton)	35

Effect of Magnet Thickness

Both material & space affect the BMR

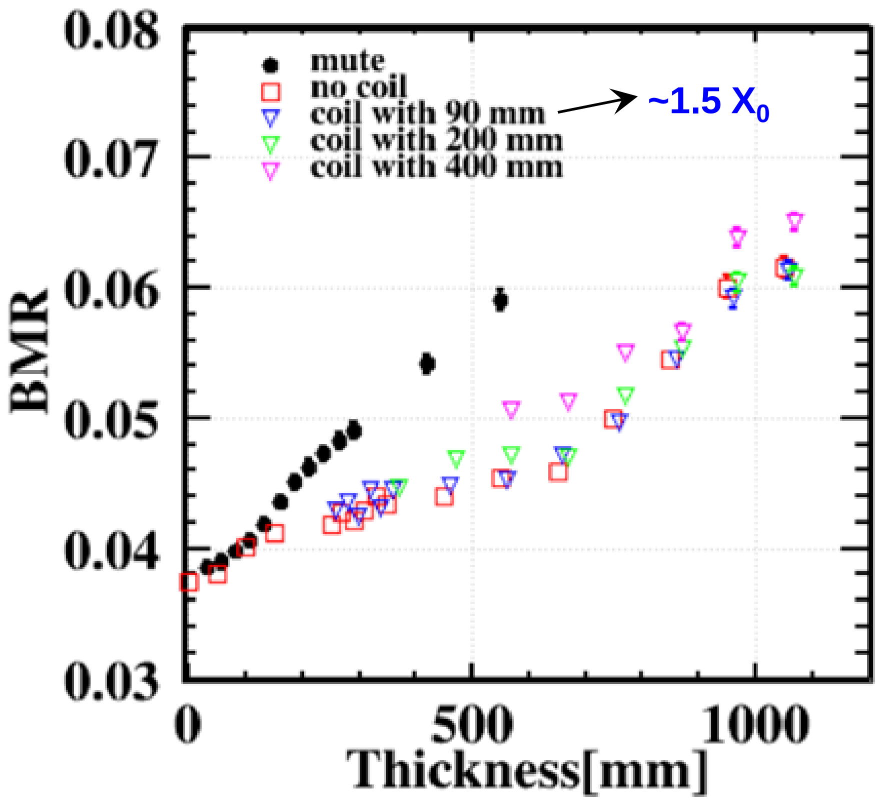

> Magnet due to polygon HCAL

Considering 2 segments of HCAL along the R direction, with the Magnet in between.

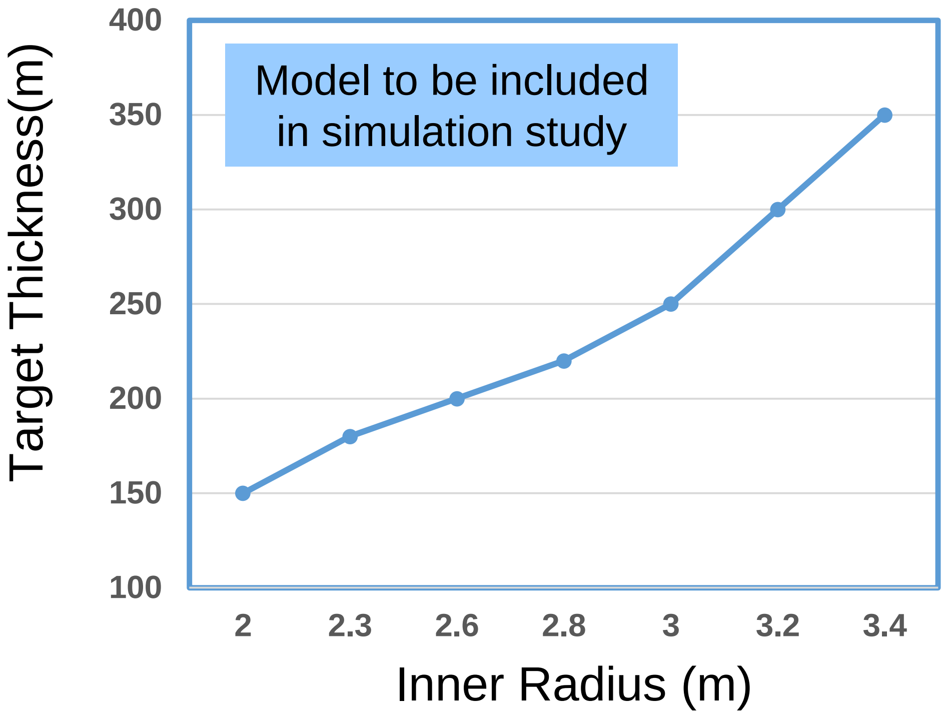

HTS Prototype Cable Development

Prototype cable: 15×10 mm^2 **,** Tape Width: 4 mm, thickness: 80 μm; tape layer: 20, Expected operating current: 6000 A@5K

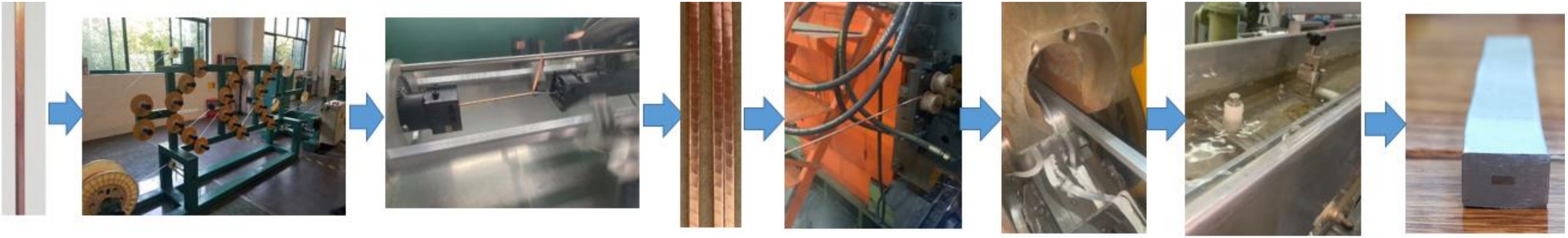

Big Progress: 10 m ASTC prototype cable is ready. Cable test is ongoing.

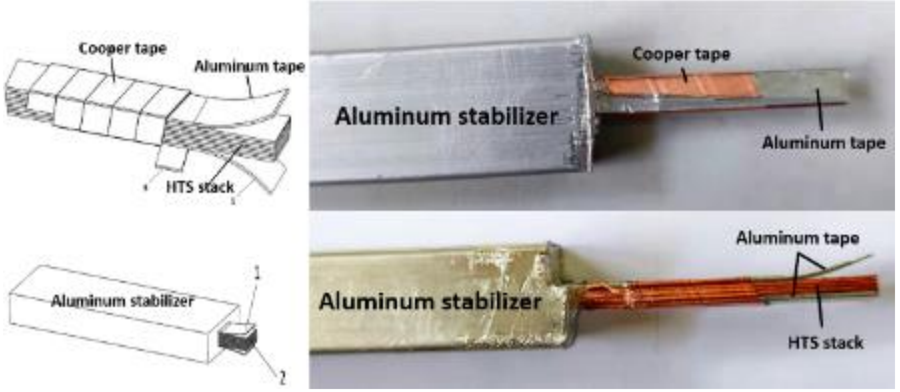

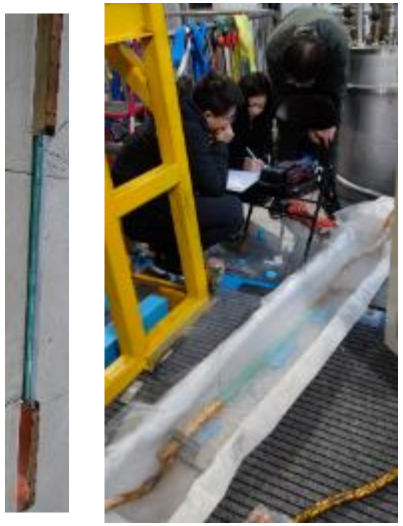

Summary

- A few new ideas of the detector technologies are being explored:
  - Drift chamber that is optimized to maximize its particle ID potential,
  - Transverse crystal bar ECAL which is also compatible with PFA,
  - PFA HCAL based on scintillation glass,
  - HTS magnet that is inside HCAL.
- A workshop on the 4th conceptual detector at Yangzhou, April 14-17, 2021. https://indico.ihep.ac.cn/event/13888/
- Busy R&D work, several papers in preparation.